Modelling CO_2 Storage in Saline Aquifers with Reactive Transport Simulator RCB

Shunping Liu

Dissertation for the degree philosophiae doctor (PhD)

at the University of Bergen

Preface

The thesis is produced as a part of the NFR project No. 801455/450224 "CO_2 capture project phase 2". The main focus of this project is to model the coupled thermal, hydraulic, geomechanical effect of CO_2 storage in saline aquifers by using reactive transport code RetrasoCodeBright.

Geological formations are currently considered the most promising carbon dioxide sequestration sites and the estimated storage capacities indicate a substantial potential for storing CO_2 in saline aquifers. A general problem is that long term predictions about underground storage security are difficult and uncertain. CO_2 injection will cause a mechanical impact due to changes in the stress field resulting from changes to the pore pressure, buoyant pressure, and volume of the rock. CO_2 may lead to significant mineral dissolution in some areas of lowered pH and mineral deposition from dissolved ions in regions of higher pH. Further, since each reservoir changes dynamically as a function of the reactive flow, the geomechanical analysis needs to be coupled to flow simulations. A survey on the current reservoir simulators on CO_2 storage has been carried in this thesis showing that for now there are no verified codes with implicit solution of reactive flow, geomechanics, and heat flow in the CO_2 storage scenarios which has been an important motivation for the choice of platform for developing a new CO_2-storage simulator, RetrasoCodeBright.

In this thesis the development and application of RetrasoCodeBright is introduced. RetrasoCodeBright is the result of coupling of two codes, Retraso, which is designed to solve the reactive transport problems and CodeBright, which is designed for the thermo-hydraulic-mechanical analysis of multiphase saline media. Code RetrasoCodeBright, briefly called RCB, has been extended for coupled hydro-thermal-geomechanical-geochemical modelling specified for CO_2 storage simulations.

The thesis consists of eight papers of which three papers are accepted or submitted to international journals; one paper is contributed in book and four papers are conference proceedings, two published and two submitted.

Acknowledgements

I take this great opportunity to thank the people who have given me help and support for my PhD study at Physics and Technology department in University of Bergen. First of all I would like to thank my supervisor, Professor Bjørn Kvamme, who has introduced CO_2 storage this interesting research topic to me. This 3-year-project is full of challenges for me who has background in informatics. Bjørn always trusts me and gives me many formal and informal lectures to explain the thermal dynamic and geo-mechanical theory to me. I owe my deepest gratitude to him.

A set of Fortran code, RetrasoCodeBright is the basic working platform for this project. To understand this code I went to Technical University of Catalunya in Barcelona and stayed there for one month in the second year of my PhD. I am thankful for Maarten Saaltink and Sebasia Olivella who have taken good care of me and explain the structures inside of the code so that I could continue on with the code and rewrite it later specially for simulating CO_2 storage processes.

I have got many helps from my colleagues in Physics and Technology department, without them I couldn't make it at last. I specially thank Lars Andreas Lågeide for his great contributes in the sensitivity studies in CO_2 storage scenarios. I am also thankful to my friend Pilvi Helina Kivela who has shared the office with me and made the working environment always pleasant for me. I would also thank the administrative and technique staffs in the institute for their great help.

After the normal three years study in University of Bergen, I began to work in Statoil AS without finishing the thesis. I am so thankful to my line manager Geir Evensen in Statoil, who supports me and helps reading the thesis. Without his great help and support the writing process would take even longer.

At last I wish to thank my family that always trust me and support me, and I am so grateful to my husband, Bowei for all his inspirational suggestions to my project and always being there for me.

Publications

Reviewed publications in scientific journals

Liu, Shunping, Kvamme, Bjørn, "*Simulating* CO_2 *Storage in Saline Aquifers with Improved code RCB*", INTERNATIONAL JOURNAL of ENERGY and ENVIRONMENT, 2007, 1, 21-27

Kvamme, B., Liu, S., *"Reactive Transport of* CO_2 *in Saline Aquifers with implicit geomechanical analysis",* 2009, Energy Procedia, 1, 3267–3274

Liu, S., Lågeide, L.A., Kvamme, B., *"Sensitivity study on storage of* CO_2 *in saline aquifer formation with fracture using reactive transport reservoir simulator RCB",* 2010, Journal of Porous Media, in press

Reviewed contributions in books

Kvamme, B., Liu, S., 2009, "*A new reactive transport reservoir simulator for aquifer storage of* CO_2 *- with implicit geomechanical analysis*" in "Carbon Dioxide Capture for Storage in Deep Geologic Formations", Volume 3, L.I. Eide (Ed.), CPL Press and BP, 2009, p. 349 - 376

Reviewed publications in conference proceedings

Liu, Shunping, Kvamme, Bjørn, "*Simulating* CO_2 *Storage in Saline Aquifers with Improved code RCB*", proceedings of the 6th WSEAS Int.Conf. on SYSTEM SCIENCE and SIMULATION in ENGINEERING, Venice, Italy, Nov. 21 – 23, 2007, 8 pages

International presentations

Liu, Shunping, Kvamme, Bjørn, "*Improved Newton Raphson Method – An Effective Tool in Solving Flow-Mechanic-Chemistry Equations of* CO_2 *Storage in Saline Aquifers*", presented at the American Conference on Applied Mathematics (MATH'08), Harvard, Massachusetts, USA, March 24th - 26th, 2008

Kvamme, Bjørn, Liu, Shunping, "*Simulating Long Term Reactive Transport of* CO_2 *in Saline Aquifers with Improved code RetrasoCodeBright*", presented at 12th International Conference of International Association for Computer Methods and Advances in Geomechanics (IACMAG) 1-6 October, 2008, Goa, India (Journal version submitted)

Kvamme, Bjørn, Shunping, Liu, "*Reactive Transport of* CO_2 *in Saline Aquifers with implicit geomechanical analysis*", presented at the 9th International Conference on

Greenhouse Gas Control Technologies (GHGT-9), 16 - 20 November 2008, Washington DC, USA

Contents

1. Introduction

Measurements of the concentrations of CO_2 and other greenhouse gases in the atmosphere show clearly the impact of the industrial revolution. The atmospheric concentration of CO_2 has increased by approximately a third from the preindustrial-age level of about 280 ppm to 370 ppm today, as a result of the burning of fossil fuels, cleaning of forests, and manufacturing of cement (Franklin M. Orr Jr., 2004). As CO_2 is the greenhouse gas that leads to the largest reduction in the reflected heat radiation from the earth, the CO_2 emissions associated with energy production is a substantial global concern. Thus, major actions are needed to reduce the accumulation of CO_2 in the atmosphere (Wigley et. al., 1996). The technology of capture and storage of CO_2 is likely to be one step towards meeting the challenge of stabilizing atmospheric CO_2 concentrations (Hoffert et al., 2002).

There are several options for underground storage of CO_2, e.g. storage in depleted oil and gas reservoirs (see e.g. Parson and Keith, 1998; Holt et al., 2000; Gale, 2003; van der Meer, 2003), storage in un-mineable coal beds, and storage in deep saline aquifers.

Parson and Keith (1998) estimate that saline aquifers have the largest storage capacity of the three options mentioned above, and they estimate the saline aquifers have a storage capacity of up to 3700 Gt CO_2. A more recent study by Gale (2003), estimate the CO_2 storage capacity of saline aquifers to be up to 10,000 Gt. These estimates inevitably involve significant uncertainties. Nevertheless, the estimated storage capacities indicate a substantial potential for storing CO_2 in deep saline aquifers. More recent publications discuss different trapping mechanisms, of which trapping as tiny bubbles is likely to keep the injected CO_2 safely stored in the briny porous rock for centuries (Juanes et al., 2009).

Additional options to the above include the use of CO_2 for enhanced oil recovery (EOR) purposes (Izgec et al., 2005) and the exchange of CO_2 with natural gas

through CO_2 injection into natural gas-hydrate reservoirs (Kvamme et. al., 2002, Graue et al., 2006, Kvamme et al., 2007). Worldwide, there are already ongoing EOR projects based on CO_2 injection. A full-scale test of hydrate storage of CO_2 through exchange with *in situ* natural hydrate will be performed in Alaska by ConocoPhillips, with partial funding from the Department of Energy (DOE).

This thesis is limited to aspects related to the storage of CO_2 in saline aquifers. Thus, the other alternatives listed above will not be discussed in further detail, although many of the features of the software developed through this work may also be useful when studying the other storage options.

1.1 Storing CO_2 in deep saline aquifers

Saline aquifers are water bearing porous-layers sandstone or limestone in the subsurface, and they are by far the volumetrically largest and most widespread proposition for large-scale CO_2 storage.

The injected CO_2 will flow through high-permeable paths and the flow will be dominated by gravity segregation. The density difference between injected CO_2 and brine will lead to a preferential flow of CO_2 towards the top of the aquifer (Kumar et al., 2005) and the CO_2 will potentially accumulate below sealing layers of clay or shale.

The injected CO_2 will also dissolve in the brine, and the mixture of brine and CO_2 will be slightly denser than the brine alone (Ennis-King and Paterson, 2003). Thus a slow vertical flow of the denser brine will cause further dilution of the dissolved CO_2.

Due to geothermal gradients and corresponding higher temperature deeper in the reservoir there is always a potential of some CO_2 to out gas again at certain depths. Other portions of the injected CO_2 may be trapped in small pores, depending on the relative wetting properties of the minerals.

Injected CO_2 imposes chemical reactions and dissolution of minerals in the regions of lowered pH. Most mineral reactions are slow (hundreds of years) while calcite and some other carbonates will dissolve in a matter of days under low pH influence close to injection. Dissolved ions, transported with the flow, may precipitate in regions of higher pH. Even though the content of rapidly dissolving carbonates may vary substantially, the distribution of these carbonates among other minerals plays a significant role. Fine distribution inside other minerals may lead to a release of smaller particles as these carbonates are dissolved. Depending on the chemical composition of the brine and the minerals present in the aquifer, some of the CO_2 may sequester as minerals (Johnson and Nitao, 2003)

1.2 The current large scale aquifer-storage projects

Currently, there are four ongoing CO_2 sequestration projects worldwide; of which two are the Sleipner and Snøhvit projects in Norway.

The Sleipner project has been running since 1996. Natural gas containing up to 9% CO_2 is produced from the Heimdal formation. Every year, one million tones of CO_2 are captured from the Sleipner natural gas and stored in a sandstone formation called Utsira, located more than 800 m below the sea floor, above the Heimdal formation. A special platform was built in order to process the natural gas, where the CO_2 is extracted and injected back into the Utsira formation.

The second CO_2 sequestration project in Norway is the Snøhvit project, located in the Barents Sea. This project is based on the liquefied natural gas (LNG) factory on the island of Melkøya. From the off-shore Snøhvit field, the natural gas is brought by pipelines to the LNG plant on Melkøya where it liquefied by cooling. Prior to the cooling the CO_2 in the natural gas is extracted and sent back to the Snøhvit field where it is injected into a sandstone formation called the Tubåen formation, located 2500 m below the sea floor and below the gas-containing layers. In this project more

than 700,000 tones of CO_2 are stored yearly. Snøhvit started production in October 2007.

In Algeria, Statoil, as well as Sonatrach and BP, are funding a CO_2 sequestration project in connection with In Salah Gas that started in 2004. In this project, CO_2 is stored in the same formation as where the natural gas is produced, but at a considerable distance away from the producing regions. Using this concept, the same caprock that keeps the natural gas from leaking will also function as a sealing for the injected CO_2. The injection volume is expected to reach 1.2 million tones per year.

The International Energy Agency (IEA) is, in the Weyburn CO_2 Monitoring and Storage Project, investigating the technical and economic feasibility of CO_2 storage in a partially depleted oil reservoir. The oil reservoir is located at Weyburn in the South-Eastern Saskatchewan, Canada, near the U.S. border between Canada and North Dakota. The primary goal of this international research project is to investigate the storage integrity of an on-shore geological storage of CO_2, during large-scale and commercial EOR operations. The final reports for Phase I were completed in mid-2004. Phase II of the project includes the continuing monitoring of the movement of CO_2 in the reservoir and the refinement of a risk/performance assessment to help determine the feasibility of CO_2 geological storage over the long term, measured in thousands of years. The IEA Weyburn project intends to demonstrate, by 2010, that CO_2-EOR is economically viable, environmentally responsible, and socially acceptable.

1.3 Geomechanical stability and CO_2 storage integrity

Of importance for aquifer-injection projects is a good characterization of the aquifer. The aquifer's regional extent, including its barriers to vertical flow, possible faults, and potential pathways for vertical migration, must be properly understood.

Furthermore, the geomechanical response to changes in fluid fluxes is one of the key questions related to storage integrity and safety of a CO_2 sequestration project. The

deep geological formations that receive and hold CO_2 are located far below fresh water aquifers and below at least one sealing formation of extremely low permeability, normally clay or shale. Slow movement deep in the Earth will cause stresses to build up within its brittle outer crust. The stress that has accumulated over hundreds to thousands of years is relieved in a few seconds and may in a worst case lead to failure and slip, which on a fault can lead to earthquakes (Foxall and Friedmann, 2008).

Effective design and implementation of geological CO_2 sequestration also requires understanding of the storage capacity of a candidate site, the impact of the different trapping mechanisms for gas in the actual reservoir and the hydrodynamics of the system (Shipton et al., 2004). In some natural CO_2 reservoirs gas leakage primarily occurs along faults and the consequences can be unpredictable. The CO_2 leakage in the Colorado Plateau off east-central Utah is one of the most dramatic examples of natural CO_2 blow out. In this reservoir the CO_2 flows upward from one or more deep sources of CO_2. These sources include the thermal de-carbonation of carbonates deep in the basin and discharges from the hydrocarbon-rich Paradox Basin. The CO_2 escapes along the Little Grand Wash and Salt Wash faults, where CO_2 charged springs and geysers, travertine and carbonate-filled veins, are localized along the fault traces. Even small fractures and faults can generate local leakage which makes these types of reservoirs unsuitable for aquifer storage. Limitations of seismic resolution can even be a limitation in the selection of appropriate storage reservoirs.

The assessment of geomechanical constraints on long term CO_2 sequestration in deep saline aquifers is discussed in Zoback's GCEP technical report 2006 "Geomechanics and CO_2 sequestration". He emphasizes the two general concerns related to the geomechanical stability of the CO_2-storage formation. The first concern is whether the injection rates can be maintained at a pressure consistent with the geomechanical constraints, i.e. at a condition where the effective stress in all principal directions is below the tensile strength of the material in these individual directions. The second concern is whether leakage and vertical migration of CO_2 can result in pressure

changes that may lead to a collapse of the cap rock. Local mineral dissolution around injection zones may also enhance the possibilities of possible sand reorganization and a corresponding collapse. These two aspects should be evaluated for all potential CO_2-sequestration formations, to assess the risk of CO_2 leakage, before committing to CO_2 disposal. Cap rock failure assessment, either tensile fracturing or shear reactivation of pre-existing fault, is therefore a key issue for preventing CO_2 leakage from deep aquifer reservoir up the surface. In this dissertation cap rock failure analysis on tensile fracturing by effective stress will be discussed in section 2.1.4.1.

CO_2 injection will cause a mechanical impact due to changes in the stress field resulting from changes to the pore pressure, buoyant pressure, and volume of the rock (Orlic, 2009). Changes in stress and the associated deformation may lead to damage of the top seal or reactivation of preexisting sealed faults, possibly leading to reduced sealing capacity of the formation. In addition to the mechanical impact on seals and faults, which may lead to leakage, the CO_2 injection may induce ground movement, which can be either aseismic, in the form of ground subsidence and/or ground uplift, or seismic. Induced seismic movement is caused by a sudden slip on the fault surfaces and discontinuities present in the subsurface. Such a movement results in an induced micro-seismic or seismic event. Unlike flow of non-reactive fluids CO_2 may, as briefly indicated above, lead to significant mineral dissolution in some areas of lowered pH and mineral deposition from dissolved ions in regions of higher pH. In view of the effects above are dynamically changing risk factors which require continuous evaluation of geomechanical stability during the injection period as well as long periods after injection period is completed. Some carbonates like calcite and magnesite dissolve rapidly while quartz and many silicates dissolve very slowly. These processes are not only dependent on the percentage of rapidly dissolving minerals, but they also depend on how the rapidly-dissolving minerals are distributed among other minerals. If the minerals are more evenly spread in a composite mineral, the dissolution may lead to fracturing of larger particles, as the "glue" of rapidly dissolving minerals disappears.

The discussion above clearly illustrates that the geomechanical properties of storage sites must be examined as a necessary part of the qualification of storage safety. Further, since each reservoir changes dynamically as a function of the reactive flow, the geomechanical analysis needs to be coupled to flow simulations. Preferably an implicit algorithm should be used to properly handle the different time scales of the various processes, including the potentially rapid reactions and instant consequences of these reactions on the geomechanical stability of the formation. This becomes even more critical in reservoirs where temperature and pressure in parts of the reservoir is inside the region where CO_2 hydrates can form. Formation of hydrate involves roughly 10% volume increase compared to liquid water and hydrate can form rapidly (microseconds to minutes).

1.4 Status of current reservoir simulators for CO_2 storage

Requirements of storage integrity are not unique for all countries in the world. In Europe there seem to be a consensus that verification of safe storage for 10,000 years is reasonable, while a corresponding time scale in USA is more on the level of hundred years or more. Common to all requirements is that the consequences are futuristic and the only possible way to "verify" the storage integrity for a selected site is by a combination of experiments and theoretical modelling at different levels. In this work the focus is limited to theoretical modelling of the reactive transport involved in CO_2 storage, with special emphasis on the coupled geochemical and geomechanical processes.

Mathematical models and numerical simulators are essential tools in addressing problems and questions that arise in the context of CO_2 storage in the deep subsurface. From the perspective of functions of reservoir simulation codes, we can divide the current codes into two categories: 1) codes that don’t include the functionality of geomechanical calculation, and 2) codes that include geomechanical calculations, either implicitly or explicitly coupled to geochemical and hydraulic calculations (Celia et al., 2005).

Codes that belong to the first category include ATHENA developed by Department of Mathematics and Department of Physics and Technology, University of Bergen; CSLS (Compositional Streamline Simulator) developed by Stanford University Petroleum Research Institute–C; and Elsa developed by Department of Civil and Environmental Engineering at Princeton University and Department of Mathematics at University of Bergen. Some other codes like GEM-GHG by Computer Modelling Group at University of Texas, MUFTE_UG by Institute of Hydraulic Engineering, University of Stuttgart and University of Heidelberg, also belong to this group that does not incorporate geomechanical effects in hydraulic, and geochemical and reactive transport calculations. This list is not complete and additional codes are available in the open community as well as internally in companies and research institutions.

Of most relevance to this project are the codes that address coupled hydro-geochemistry-geomechanics problems. During a literature survey we found that the list of codes that include geomechanics is more limited, at least within open codes and/or published codes. These codes are NUFT/LDEC, developed at Lawrence Livermore National Laboratory (LLNL); DYNAFLOW, developed by Princeton University; and TOUGH-FLAC developed at Lawrence Berkeley National Laboratory.

To our knowledge, or at least what was available in open scientific literature, there are no publications related to simulations of CO_2 storage, where DYNAFLOW is applied to problems that cover modelling of both reactive-transport and geomechanics.

NUFT is currently a flow/transport-only version and contains no reactive chemistry. In NUFT/LDEC explicit account is taken of the coupling between geochemical and geomechanical process by dependence of permeability on porosity change.

The TOUGH-FLAC simulator (Rutqvist et al., 2002) is based on a coupling of the two existing computer codes TOUGH2 (Pruess et al., 1999) and FLAC3D (Itasca

Consulting Group, 1997). TOUGH2 was developed for geo-hydrological analysis with multiphase, multi-component fluid flow and heat transport, while FLAC3D is designed for estimation of rock and soil mechanics. The TOUGH2 and FLAC3D are linked through external coupling modules. Moreover, TOUGH-FLAC has not been coupled with chemical reactive transport modelling. There is a reactive transport version of TOUGH called TOUGHREACT but no published literature on extended version of TOUGHREACT coupled with geo-mechanics is found.

A more recent benchmark study on CO_2 storage in geological formations (Class et al., 2009) compares the current models by their simulation results from a synthetic example. Results show that different models give divergent description and prediction on CO_2 migration. The study reveals that different models have different interpretation of the given conditions, by using different assumptions and simplifications, and also significant differences in their numerical performance. There is undoubtedly a need to improve existing codes and/or develop new numerical simulation tools that are capable to, more rigorously, incorporate the different trapping mechanisms. Furthermore, due to the many different time scales involved in the processes related to CO_2 storage in geological formations (CO_2 dissolution, dissociation, and reactions), implicit couplings of flow transport, chemical reactions, and geomechanics, is desirable.

Some relevant reservoirs for storage of CO_2 have zones of low temperatures and sufficient pressure to result in the formation of hydrates from CO_2 and water. The increased volume of hydrates compared to liquid water, imposes a potential local geomechanical issue. The process of hydrate formation is very fast, typically seconds to minutes (Kvamme et al., 2007). The hydrate dynamics is even more complex since formed hydrate may dissociate towards under-saturated water in contact with mineral surfaces. Stresses induced by formation and dissociation of hydrates are therefore clearly an issue that requires an implicit solution due to the short time scales of these dynamic processes.

In view of the above discussion it appears that even today there are no verified codes with implicit solution of reactive flow, geomechanics, and heat flow, and this has been an important motivation for the choice of platform for developing a new CO_2-storage simulator.

2. RetrasoCodeBright (RCB)

RetrasoCodeBright (RCB) is the result of a coupling of two codes: CodeBright and Retraso. CodeBright (COupled DEformormation of BRIne Gas and Heat Transport) was designed for the thermo-hydraulic-mechanical analysis of three-dimensional multiphase saline media (Olivella et al., 1996). Retraso (REactive TRAnsport of SOlutes) is a code for solving two-dimensional reactive transport problems (Saaltink et al., 1997). The combination of the two codes is aimed to model complex problems consisting of coupled thermal, hydraulic, geomechanical, and geochemical processes. The two parts of the code will be separately introduced in this section.

2.1 CodeBright

CodeBright has its independent history of applications and corresponding publications from different case studies, and the code is still being used independently for non-reactive systems. A brief summary from a literature survey on applications of the code is given in Section 2.1.1. In Section 2.1.2 we give a more detailed description of the governing equations of CodeBright. The numerical approach for mechanical problems is dictated in section 2.1.3, while different rock-failure criteria and the failure equation used in CodeBright is described in section 2.1.4.

2.1.1 Introduction and some applications of CodeBright

CodeBright was originally developed to model the long-term behaviour of a sealing system for the assess galleries of high-level radioactive-waste repositories in rock salt. In rock-salt systems, long-term sealing is sometimes ensured by crushed salt bricks, which become nearly impervious under the compression by the overlaying rocks. However, the basic nature of the investigations makes the results applicable well beyond their original motivation (Olivella, 1996). CodeBright couples the

thermal (multiphase heat transport in porous media), hydraulic (two phase flow of liquid and gas in porous media including vapour), mechanical (unsaturated soil mechanics under isothermal conditions), problems and the solute transport. A number of improvements have been made to the code since its early development (Olivella et al., 1996). One of them is the construction/excavation that is handled by activating and deactivating sub domains (Olivella et al., 2008).

CodeBright has so far been applied to study different geotechnical engineering problems at the Department of Geotechnical Engineering and Geosciences at UPC-BARCELONA TECH (UPC) in Barcelona.

Olivella and Gens (2005) reported on the environmental impact from storage of radioactive waste in unsaturated rock. Temperature up to 200°C implies evaporation of water around the drift in amounts sufficiently high to result in out drying of the rock. The different properties of the rock matrix and the rock fractures produce different de-saturation of the pores and correspondingly different permeability. The heating also induces volumetric (compressive and dilative) changes and shear deformation in the rock. These deformations result in changes of the intrinsic permeability. As such both hydraulic and mechanical processes lead to changes in the permeability that affect the flow of water and gas, which in turn influences the heat transport and the temperature.

Alonso et al., (2005) discussed improved consititutive modelling of rockfill as applied to the Beliche Dam in Algarve (Portugal). This is a a zoned earth dam with rockfill shoulders and a central clay core which experienced large collapse settlements due to reservoir impounding and direct action of rainfall. Long-term field records of vertical and horizontal displacements are available as well as a set of large scale laboratory tests on rockfill specimens. Several previous numerical analyses had failed to capture the relevant effect of weather conditions on the behaviour of the dam. This study was the first published numerical study that was able to capture a more complete history of dam constructions, impoundment and rainfall using the coupled flow-deformation model CodeBright. Deformations during construction and

impoundment have been reproduced. In general, long-term deformations are controlled by the varying wetting history of the dam shoulders and by an intrinsic deformations component. The wetting action comes to an end when the relative humidity of the rockfill reaches 100% for the first time. The paper also discusses scale effects and the role of rockfill permeability in the development of deformation.

CodeBright was also used by Olivella and Alonso (2004) to model a case related to disposal of radioactive waste. The Gas Migration Test (GMT) at the Grimsel Test Site (GTS) underground laboratory in central Switzerland was designed to investigate gas migration through an Engineered Barrier System (EBS). The EBS consists of a concrete silo embedded in a sand/bentonite buffer emplaced in silo cavern that intersects a shear zone in the surrounding granite host rock. The GMT was operated by the National Cooperative for the Disposal of Radioactive Waste (NAGRA) and the modelling studies have used coupled two-phase geomechanical codes, CodeBright. Gas generated in the waste can migrate by diffusion and advection. In the case of two-phase flow, the generated pore pressure may reach sufficient levels to induce opening of discontinuities. In the gas injection test phase the inferred pressure-dependent permeability change no longer strictly corresponds to an effective stress change because the pressure in the upper cavern and the total stress in the EBS increase. However, the pressure-dependent permeability increases along the interfaces which may correspond changes in the minimum effective stress at the top of the silo and minimum horizontal stress at the granite interface.

Simulation of coupled problems is also carried out for laboratory experiments. Harrington and Horseman (2003) use CodeBright to model the injection of gas in initially saturated soil with permeability variations induced by changes in the degree of saturation and deformation.

Garitte et al. (2008) show analyses for placing heat sources in the Callovo-Oxfordian mudstone, in order to study the intrinsic thermal properties of the rock and to examine the thermo-hydro-mechanical (THM) couplings. An experiment will be launched after the excavation of the GED gallery, an extension of the existing GMR

gallery. The excavation of a small niche is planned in the GED drift, from which the heater boreholes and instrumentation boreholes will be drilled. One of the objectives of the design work is also the determination of the optimal instrumentation pattern.

2.1.2 The governing equations

CodeBright is a numerical finite-element model for non-isothermal multiphase flow of brine and gas through porous deformable saline media. The governing equations for non-isothermal multiphase flow of water and gas, through porous and deformable saline media, are presented by Olivella et al., 1996. The equations can be categorized into four major groups, i.e. balance equations, constitutive equations, equilibrium relationships, and definition constraints.

Equations for mass balance are established following the compositional approach. That is, mass balance is performed for water, gas, and salt, rather than using phases of solid, liquid, and gas. An equation for the balance of energy is established for the medium as a whole. The momentum-balance equation for the porous medium is reduced to that of stress equilibrium. These equations give a full description of the hydro-thermo-mechanical state of the medium, in terms of the velocity u of the solid in three spatial dimensions, the liquid pressure P_l, the gas pressure P_g, and the temperature T.

The mass balance of the solid is given by

$$\frac{\partial}{\partial t}(\theta_s(1-\phi)) + \nabla \bullet (j_s) = 0 \tag{1}$$

where θ_s is the mass of the solid per unit volume, j_s is the flux of solid and ϕ is porosity. From this equation, an expression for porosity variation is obtained as

$$\frac{D_s\phi}{Dt} = \frac{1}{\theta_s}[(1-\phi)\frac{D_s\theta_s}{Dt}] + (1-\phi)\nabla \bullet \frac{du}{dt} \tag{2}$$

where $u = (u_x, u_y, u_z)$ is the vector of solid displacements.

The water mass balance is described by

$$\frac{\partial}{\partial t}(\theta_l^w S_l \phi + \theta_g^w S_g \phi) + \nabla \bullet (j_l^w + j_g^w) = f^w \tag{3}$$

where θ_l^w and θ_g^w are respectively the mass fraction of water in liquid and gas phases, while *Sl* and *Sg* are the degrees of saturation of the liquid and gaseous phases, i.e. the fraction of pore volume occupied by each phase, and f^w is the external supply of water.

The gas mass balance is described by

$$\phi \frac{D_s(\theta_l^a S_l + \theta_g^a S_g)}{Dt} + (\theta_l^a S_l + \theta_g^a S_g)\frac{D_s \phi}{Dt} + ((\theta_l^a S_l + \theta_g^a S_g)\phi)\nabla \bullet \frac{du}{dt} + \nabla \bullet (j_l^{'a} + j_g^{'a}) = f^a \tag{4}$$

where θ_l^a and θ_g^a are respectively the masses of gas in liquid and gaseous phases, $j_l^{'a}$ and $j_g^{'a}$ are the total mass fluxes of gas in liquid and gaseous phases relative to the solid phases, and f^a is gas supply.

The balance of momentum for the porous medium reduces to the equilibrium equation for macroscopic total stresses if the inertial terms are neglected (Bear and Bachmat, 1986):

$$\nabla \bullet \sigma + b = 0 \tag{5}$$

where σ is the stress tensor and b is the vector of body forces. The assumption that the inertial terms can be neglected is usually accepted, because both velocities and accelerations are small, resulting in inertial terms that are negligible in comparison with the stress terms. Bear and Bachmat (1986) also show that under certain simplifications, the Terzaghi's concept of effective stress, i.e. the total stress minus fluid pressure for saturated conditions (Terzaghi, 1925), can be obtained. Providing an adequate mechanical constitutive model, the equilibrium equation is

transformed into a form, in terms of the solid velocities, fluid pressures, and temperature. A possible decomposition of the strains is

$$\dot{\varepsilon} = \dot{\varepsilon}^{e} + \dot{\varepsilon}^{vp} + \dot{\varepsilon}^{c} + \dot{\varepsilon}^{o} \tag{6}$$

where $\dot{\varepsilon}^{e}$ is the elastic strain rate due to stress, $\dot{\varepsilon}^{vp}$ is the viscoplastic strain rate (except creep), $\dot{\varepsilon}^{c}$ is the creep strain rate, and $\dot{\varepsilon}^{o}$ is the deformation due to temperature or fluid pressure changes. Hence, $\dot{\varepsilon}$ is the total strain rate, which is related to solid velocities through the compatibility conditions, which can be written as

$$\dot{\varepsilon} = \frac{1}{2}(\nabla \dot{u} + \nabla \dot{u}^{t}) \tag{7}$$

where $\dot{u}$ and $\dot{u}^{t}$ is respectively the net and total solid-velocity vector.

Obviously, the simplest description for a porous material is the elastic one, written as

$\dot{\varepsilon} = C^{e}\dot{\sigma}$, where $\dot{\sigma}$ is the stress-rate tensor and C^{e} is the elastic compliance matrix (inverse of the stiffness matrix).

The equation for internal energy balance for the porous medium is established taking into account the internal energy in each of the phases *Es, El,* and *Eg*,

$$\frac{\partial}{\partial t}(E_s\rho_s(1-\phi) + E_l\rho_l S_l\phi + E_g\rho_g S_g\phi) + \nabla\bullet(i_c + j_{Es} + j_{El} + j_{Eg}) = f^{Q} \tag{8}$$

where i_c is the energy flux due to conduction through the porous medium, the fluxes (j_{Es}, j_{El}, j_{Eg}) are advective fluxes of energy caused by mass motions, and f^{Q} is an internal/external energy supply. In this case, this source term accounts, for instance, for energy dissipation due to deformation of the medium, which is negligible in most cases. The use of the material derivative allows for obtaining an equation formally

similar to the mass balance for water. The reason for the similarity is that both water and internal energy are considered present in the three phases.

2.1.3 Computational approach for coupled Thermo-Hydro-Mechanical problems

This section is divided into two subsections in which the first sub-section describes the mechanical problem and integration algorithms while the second sub-section is devoted to the handling of the mass and energy balance equations. The partial differential equations together with constitutive laws are strongly coupled and nonlinear. In section 2.1.3.1 the mechanical constitutive model is discretized. This produces a vectorial nonlinear function to be accomplished at every grid point of the medium. In section 2.1.3.2 the model is incorporated in the equation of equilibrium of stresses. The Newton-Raphson method is used to obtain an iterative scheme to solve for the nonlinearities. Details about the treatment of the different terms (accumulation, advective and nonadvective fluxes and volumetric strain) are presented in section 2.1.3.3. The Newton-Raphson method is applied to the residual form of these mass and energy equation.

2.1.3.1 Discrized form of the linear elastic-mechanic model

In Section 2.1.2 the general model to reproduce the stress-strain behaviour is shown as Equation (6). The assumption of only elasticity deformations is, from a numerically point of view, convenient and practical for CO_2-storage scenarios. An elastic linear model for the instantaneous deformation is written as

$$\dot{\varepsilon} = \dot{\varepsilon}^{e}(\dot{\sigma}', \dot{s}, \dot{T}, e) , \tag{9}$$

where $\dot{\sigma}'$ is the effective stress-rate tensor, s is the difference between gas and liquid pressure, $\dot{T}$ is the rate of temperature change, and e is the void ratio. Equation (9) expresses that the strain rate depends on the rate of stress, the rate of

variation of the difference between gas and liquid pressures, and the rate of temperature variations.

If strain is written in terms of the displacement-field u, and a finite difference along time is performed, Equation (9) can be rewritten as

$$h^{k+1} = -B\Delta^k u + \Delta^k \overset{\bullet e}{\varepsilon} + m\beta\Delta^k T = 0 \tag{10}$$

where B is a tensor of spatial derivatives that transforms the displacement component u into the strain components ε, Δ^k represents an increment between time t^k and t^{k+1}, $\Delta^k \overset{\bullet e}{\varepsilon}$ is an increment of the elastic strain, m is an auxiliary vector defined as $m^T = (1,1,1,0,0,0)$, and β is a thermal expansion coefficient (the thermal expansion is assumed to be linear). Thus, h^{k+1} is a nonlinear function of stresses, fluid pressure, temperature, void ratio, and displacements. At each point of the medium, this function should vanish in order for the material to behave according to the constitutive equations (Olivella, 1995).

2.1.3.2 Mechanical problem analysis

The weighted residual method is applied to the stress equilibrium Equation (5) by the Green's theorem, which can be written as

$$r(\sigma^{k+1}) = \int_v B^T \sigma^{k+1} dv - b^{k+1} = 0 \tag{11}$$

where $r(\sigma^{k+1})$ represents the residual corresponding to the mechanical problem and σ^{k+1} is the stress vector at time t^{k+1}. The matrix B is defined in a way such that the stress is formally a vector and not a tensor. The body-force terms and the boundary-traction terms are both represented by the vector b^{k+1}.

The Newton-Raphson method is used to solve Equation (11). The vector of residuals at the nodal points should vanish at the next iteration $(l+1)$, thus using a Taylor expansion of the residual gives

$$r^{l+1} = r^l + \int_v B^T(\sigma^{l+1} - \sigma^l)dv = 0\,. \tag{12}$$

Further, by introducing a Taylor expansion of the constitutive Equation (10) with respect to the independent variables u, P_g, P_l, and T, the equation becomes

$$h^{l+1} = h^l + \frac{\partial h^l}{\partial \sigma}(\sigma^{l+1} - \sigma^l) + \frac{\partial h^l}{\partial u}(u^{l+1} - u^l) + \frac{\partial h^l}{\partial P_g}(P_g{}^{l+1} - P_g{}^l) + \frac{\partial h^l}{\partial P_l}(P_l^{l+1} - P_l^l) + \frac{\partial h^l}{\partial T}(T^{l+1} - T^l) = 0 \tag{13}$$

where the superscript l refers to the iteration process. Equation (13) allows us to obtain the stress correction at any point in the continuum as:

$$\sigma^{l+1} - \sigma^l = -D(h^l + \frac{\partial h^l}{\partial u}(u^{l+1} - u^l) + \frac{\partial h^l}{\partial P_g}(P_g{}^{l+1} - P_g{}^l) + \frac{\partial h^l}{\partial P_l}(P_l^{l+1} - P_l^l) + \frac{\partial h^l}{\partial T}(T^{l+1} - T^l)) \tag{14}$$

where the stiffness matrix for elasticity is defined as $D = (\frac{\partial h^l}{\partial \sigma})^{-1} = D^e$.

Combination of Equations (12) and (14) leads to:

$$\begin{aligned} &\int_v B^T DB(u^{l+1} - u^l)dv + \int_v B^T D\frac{\partial h^l}{\partial P_g}(P_g{}^{l+1} - P_g{}^l)dv + \int_v B^T D\frac{\partial h^l}{\partial P_l}(P_l^{l+1} - P_l^l)dv + \\ &+ \int_v B^T D\frac{\partial h^l}{\partial T}(T^{l+1} - T^l)dv = -r^l - \int_v B^T Dh^l dv \end{aligned} \tag{15}$$

where $\partial h^l / \partial u = B$. Thus, the residual r is expressed by two terms; the equilibrium of stresses and the constitutive equations which should be accomplished at every point.

2.1.3.3 Mass and energy balance equations

It is assumed that the weighted-residual method is applied followed by the use of Green's theorem. After doing so, the discrete form of the equations is obtained, every equation representing the balance in a cell associated to a node. Four main types of mass and energy balances can be distinguished among the terms in each balance equation. In order to explain details of the numerical treatment of mass and energy

balance equations, the water mass balance equation is used as an example (Olivella, 1995).

Type 1: Storage changes of mass or energy at constant porosity is described by

$$\int_e N_i \phi \frac{D_s(\theta_g^w S_g)}{Dt} dv \approx \int_e N_i \phi \frac{\partial(\theta_g^w S_g)}{\partial t} dv = \int_e N_i \phi^k \frac{\Delta^k(\theta_g^w S_g)}{\Delta^k t} dv \tag{16}$$

where the integral over the element e represents the contribution of node i (see Figure 1). Equation (16) describes that the material derivative with respect to the solid velocities is approximated and represented as a time derivative by assuming that the advective terms caused by the solid motion are small. A finite difference approximation in time is then introduced for the partial derivative. It should be computed only once for a given mesh, which gives rise to a concentrated matrix, i.e., the storage corresponding to node i only depends on state variables at this node.

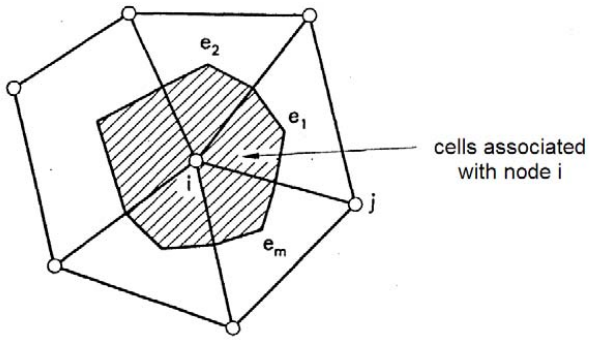

Fig. 1 Representation of a cell in a finite element mesh

Type 2: Advective flux due to phase motion:

$$\begin{aligned} &-\int_e \nabla^T N_i \theta_g^w q_g dv = [\int_e \nabla^T N_i k^k (\frac{k_{rg}}{\mu_g} \theta_g^w)^{k+\varepsilon} \nabla N_j dv](P_g)_j^{k+\theta} - \\ &-\int_e \nabla^T N_i k^k (\frac{k_{rg}}{\mu_g} \theta_g^w \rho_g)^{k+\varepsilon} g dv \end{aligned} \tag{17}$$

where j indicates a sum over the element nodes and $k+\varepsilon$ and $k+\theta$ are two different intermediate time points between t^k and t^{k+1}. A generalized Darcy's law is used and written as

$$q_g = -\frac{kk_{rg}}{\mu_g}(\nabla P_g - \rho_g g) \tag{18}$$

where k is the tensor of intrinsic permeability, k_{rg} is the relative permeability of the gas phase, μ_g is the dynamic viscosity of gas, and g is a vector of gravity forces. All the variables that appear inside the integral are considered element-wise.

Type 3: The nonadvective flux due to motion of species is written

$$-\int_e \nabla^T N_i i_g^w dv = [\int \nabla^T N_i (\phi\tau)^k (\rho_g S_g D_g^w)^{k+\varepsilon} I \nabla N_j dv](\omega_g^w)_j^{k+\theta} \tag{19}$$

where j indicates a sum over the element nodes. Fick's law is also used and can be written as:

$$i_g^w = -\phi\tau\rho_g S_g D_g^w I \nabla \omega_g^w \tag{20}$$

where τ is a tortuosity parameter, D_g^w is the molecular diffusion coefficient, which is a function of temperature and gas pressure, and I is the identity matrix. Here, a diffusive term is used. The tensor of mechanical dispersion is defined in terms of phase velocities, which are also considered element-wise, and is computed at the intermediated time $t^{k+\varepsilon}$.

Type 4: storage changes caused by volumetric deformation of the medium

$$\begin{aligned}&\int_e N_i(\theta_g^w S_g \frac{\theta_s^h}{\theta_s^h - \theta_l^h S_l})\nabla \bullet \dot{u}\, dv = \int_e N_i(\theta_g^w S_g)^{k+\varepsilon} m^T B \dot{u}\, dv = \\ &= [\int_e N_i(\theta_g^w S_g)^{k+\varepsilon} m^T B_j dv]\frac{(\Delta^k u)_j}{\Delta^k t}\end{aligned} \tag{21}$$

where j indicates a sum over element nodes and B_j is the sub matrix j of B.

With all terms transformed into their discrete forms, the partial differential equations are converted into a set of nodal balance equations.

2.1.4 Uncertainties in caprock failure assessment

Deep aquifers are open geological systems which commonly lack structural confinement; cap rock layers are sealing and confining geological units for such CO_2 geological storage sites (Rohmer and Bouc, 2010). The CO_2-injection operations lead to an increase in the reservoir fluid pressure and changes in mechanical stresses that might potentially induce creation of new fractures or reactivation of pre-existing faults in the cap rock layers (Hawkes et al., 2005; Rutqvist et al., 2007, 2008; Vidal-Gilbert et al., 2009). These mechanical discontinuities represent leakage pathways (Wiprut and Zoback, 2000) for CO_2 to escape from the deep aquifer reservoir, hence generating potential risks for the humans and environment (Holloway, 1997), and also reducing the efficiency of the storage to mitigate climate change. From a practical point of view, cap rock-failure assessment is carried out using predictive models which involves a large number of parameters. The models are correspondingly computationally time consuming (Rohmer and Bouc, 2010). Replacing the complex model by a simplified analytical model is an alternative which can be solved easily and fast (Bouc et al., 2009).

Section 2.1.4.1 gives an overview of the conventional approach for caprock failure assessment. The failure criteria used in the CodeBright module is introduced in Section 2.1.4.2.

2.1.4.1 Caprock failure assessment by the effective stress σ_{ij}'

To study geomechanics of the system, effective stress calculation has been implemented into RCB according to Terzaghi's Principle (Terzaghi, 1943). According to this principle, effective stress controls the mechanical failure of rock and is defined as:

$$\sigma_{ij}' = \sigma_{ij} - P\delta_{ij} \tag{22}$$

where δ is the Kronecker symbol ($\delta_{ij} = 0$ if $i \neq j$ and $\delta_{ij} = 1$ otherwise), P is pore pressure and σ is the total stress.

According to this definition, a tensile fracture will happen if the minimal effective stress is negative and its absolute value is greater than tensile strength of the formation:

$\sigma'_m < 0$ & $|\sigma'_m| > \tau$, where σ'_m is minimal effective stress and τ is Tensile strength.

CO_2 injection will lead to an increase in the pore pressure inside and around the host reservoir that results in a general decrease of the effective stress (Hawkes et al., 2005; Rutqvist et al., 2007, 2008; Vidal-Gilbert et al., 2009). Two main mechanical failure mechanisms must be taken into account when predicting the performance of a particular site for CO_2 sequestration (Rutqvist et al., 2007, 2008), i.e., tensile fracturing and shear-slip reactivation of pre-existing fractures and faults.

2.1.4.1.1 Tensile fracturing

A tensile fracture can be induced provided that the minimal effective stress $\sigma_{\min}'$ becomes negative (compressive stress is positive by convention) and its absolute magnitude exceeds the tensile strength either of the rock matrix or of the fracture R_T. In risk management, we consider that the most critical tensile fracture is vertical, as it represents a direct conduit from the host reservoir to the surface (Rohmer and Bouc, 2010). The tensile failure criterion F_t is defined such that $\sigma_{\min}' = \sigma_h'$, i.e.,

$$F_t(R_T, \sigma_h') = -(R_T + \sigma_h') \quad (23)$$

Tensile fracturing appears if $F_t \geq 0$.

2.1.4.1.2 Shear slip fault reactivation

The potential for shear slip along pre-existing faults or fractures can be defined based on the Coulomb criterion, using the maximum shear stress τ, which acts along the

fault plane and on the mean effective stress σ_m' (Jaeger and Cook, 1969). We assume that a cohesion less fault can exit at any point of the studied zone and with an arbitrary orientation, following the methodology described in (Rutqvist et al., 2007, 2008). The Coulomb criterion can be written in the principal stress plane (Jaeger and Cook, 1969) as

$$|\tau| = \sigma_m' \sin(\varphi') + c' \cos(\varphi')$$

where c' is the fault coefficient of internal cohesion and φ' is the fault angle of internal friction. In the present study, we consider that the most critical faults are cohesion less, i.e. $c' = 0$, hence the shear-slip failure criterion F_s is defined such that $\sigma_3' = \sigma_h'$ and $\sigma_1' = \sigma_v'$ as follows:

$$F_s(\varphi', \sigma_h', \sigma_v') = (\sigma_v' - \sigma_h') - (\sigma_v' + \sigma_h') \sin(\varphi') \tag{24}$$

A pre-existing cohesion less fault is reactivated if $F_s \geq 0$.

2.1.4.2 The failure criteria

A major challenge in estimating the capacity of reservoirs/aquifers for geological storage of CO_2 is the geological heterogeneity in the reservoir, in particular the presence of sub-seismic fractures, faults, and deformation structures. CO_2 injection increases the fluid pressure, which leads to changes in the stress state of the reservoir and also in the sealing rocks above and below the reservoir. Under high strain rates, sealing rocks may become brittle but it is difficult to establish general failure criteria. The use of empirical criteria requires attention to the original conditions and systems they were derived from and limitations in extrapolability (Olivella, 1994).

The general form for computation of fracture strains is written as

$$\dot{\varepsilon}_{ij}^{f} = \frac{1}{\eta} < F > \frac{\partial F}{\partial \sigma_{ij}} \tag{25}$$

where $F = F(I_1, I_2)$ is the extended Drucker-Prager criterion (Drucker and Prager, 1952) where $< F >$ equals 0 if $F \leq 0$ and equals F, otherwise. Here $\dot{\varepsilon}_{ij}^{f}$ is the strain-rate tensor at failure, I_1 is the first invariant of the stress tensor, J_2 is the second invariant of the deviatoric stress tensor, and η is a viscous parameter that may depend on the state variables.

The extended Drucker-Prager criterion is given by Hunsche and Albrecht (1990). The criterion is a function of a failure octahedral shear stress, which is temperature dependent, octahedral normal stress, and Lode's parameter. Hambley et al (1989) propose a combined failure criterion. Juvinal and Marshek (1991) pointed out that this criterion is an extension of the Mohr-Coulomb criterion. Colmenares and Zoback (2002), examined seven different failure criteria by minimizing the mean standard deviation between the predicted failure stress and corresponding experimental data for five different rock types at a variety of stress states. They find that the polyaxial criterium, the Modified Wiebols and Cook criterium, and the Modified Lade criterium all achieve a good fit to most of the test data.

Among the available mechanical constitutive laws, the thermo-elastoplastic law is based on the Basic Barcelona Model (Alonso et al. 1990) which was developed to describe the hydro-mechanical behaviour of partially saturated soils. The relevance of this model for highly expansive clays is investigated. An extension of the Mohr-Coulomb failure criteria for partial saturated soil has been used to model stress-strain behaviour in CodeBright.

2.2 Retraso

A brief literature survey on the use of the RetrasoCodeBright is given in section 2.2.1, followed by a more detailed description of the Retraso part of the code in Section 2.2.2.

2.2.1 Introduction of Retraso

Retraso models the interactions between transport processes and chemical reactions of solutes in the groundwater. The transport processes include advection, dispersion, and diffusion. Chemical reactions include acid-base reactions, redox reactions, complexation, biodegradation, adsorption, cation exchange, and precipitation/dissolution of minerals. The simulator is therefore capable of describing the main processes which are relevant for soil and groundwater contamination problems, including studies of groundwater quality and water-rock interaction.

In a study on the impact of a mine-tailing spill at Aznalcóllar in south-western Spain Saaltink et al. (2002) investigate the oxidation of pyrite and other sulphides using a two column experiments and reactive transport modelling. The columns were filled with pyritic sludge mixed up with a sandy and a clayey soil, respectively. Prior to simulating reactive transport, the flow model, CodeBright, is applied which permitted a detailed description of the behaviour of the column at a daily time scale. The most important parameter extracted was the hydraulic saturation. This parameter controlled the amount of O_2 that could diffuse into the soil, which affected the rate of pyrite oxidation. Two types of models were developed: (1) transient flow and heat transport without solute transport and chemical reactions; and (2) steady-state flow and reactive transport. The sandy and clayey columns behaved very differently. Finally, the model was used to predict the behaviour of other soil types and other sludge contents.

The alluvial deposits of the Agrio River, in south-western Spain, are studied using terrace mapping, boreholes, trenching, and vertical electrical sounding, to select an adequate location for a permeable reactive barrier. Permeable Reactive Barriers (PRBs) are deep trenches excavated into an aquifer and filled with a permeable material that causes pollutants to either degrade or precipitate. Design of the reactive-barrier material is aided by laboratory column experiments. These experiments are qualitatively reproduced by means of Retraso (Salvany, et al. 2004), which allows for

simulation of the long-term behaviour of the barrier, and also support the design of the width of the PRB.

There has been considerable progress on reactive transport modelling during the last twenty years. Reactive transport involves many chemical species that together undergo complex interactions and chemical reactions. Saaltink et al. (1998) used algebraic manipulations to reduce the number of variables to the minimum, i.e. to the actual degrees of freedom according to the phase rule. As algorithm for solving the highly non-linear mathematical equations for reactive transport in Retraso the one-step global implicit, or Direct Substitution Approach in implemented. In the algorithm chemical equations and transport equations are solved separately. One, two, and three-dimensional finite elements can be used for the spatial discretization.

2.2.2 The governing equations

Aqueous complexation reactions

The continuous motions of dissolved ions, together with their large number per unit volume that causes numerous collisions, make the formation of ion pairs and dissolved complexes possible. Since these reactions are almost instantaneous, they can be effectively considered as equilibrium reactions, i.e.

$$\log K_a = S_a \log c_a + S_a \log \gamma_a(c_a) \tag{26}$$

where K_a is the equilibrium-constant vector, which only depends on temperature and pressure, S_a is the stoichiometric coefficient matrix for aqueous complexation reactions, c_a is the molar concentration vector of aqueous species, and γ_a is the vector of thermodynamic activity coefficients.

Gas-liquid interactions under equilibrium conditions

Assuming that all gas-liquid reactions are sufficiently fast with respect to the flow, the equilibrium condition is

$$\log p_f = -\log K_f - \log \gamma_f + S_f \log c_{a1} + S_f \log \gamma_{a1} \tag{27}$$

where p_f is the vector of partial pressure of the gas species in the gas phase, γ_f is the vector of activity coefficients for gas, S_f is the submatrix of stoichiometric coefficients for the gas-dissolution reactions $(N_f \times N_{a1})$, and K_f is the vector of equilibrium constants (Saaltink et al., 2005).

Solid-liquid interactions under equilibrium conditions

Under equilibrium conditions, dissolution-precipitation reactions can be described as

$$\log X_m + \log \gamma_m + \log K_m = S_m \log c_{a1} + S_m \log \gamma_{a1} \tag{28}$$

where X_m is the vector of molar fraction of the m th species in a solid phase, with its thermodynamic activity coefficient γ_m, S_m is the submatrix of stoichiometric coefficients of the dissolution reactions ($N_m \times N_{a1}$, with N_m being the number of minerals), and K_m is the vector of equilibrium constant.

Kinetic rate laws

In RetrasoCodeBright, the rates of mineral dissolution or precipitation, is calculated according to the general expression of Lasaga (1984)

$$r_m = \sigma_m \zeta_m \exp\left(\frac{E_{a,m}}{RT}\right) \sum_{k=1}^{N_k} k_{mk} \prod_{i=1}^{Ns} acc_i^{P_{mki}} \left(\Omega_m^{\theta_{mk}} - 1\right)^{\eta_{mk}} \tag{29}$$

where r_m is the mineral dissolution rate (moles of mineral per volume of rock and unit time), k_m is the experimental rate constant (in the same units). The saturation ration Ω_m is the ratio between the ion-activity product and the solubility product,

$$\Omega_m = \frac{1}{K_m} \prod_{i=1}^{Nc} a_{i,actual}^{v_{mi}} \tag{30}$$

where

$$K_m = \prod_{i=1}^{N_C} a_i^{\nu_{mi}} = \prod_{i=1}^{N_C} c_i^{\nu_{mi}} \gamma_i^{\nu_{mi}} \tag{31}$$

The log Ω_m value is known as the saturation index SI_m. The system reaches the minimum free energy at equilibrium when $\Omega_m = 1$ or $SI_m = 0$. The parameters θ and η must be determined from experiments. The term inside the parenthesis in Equation (29) are called the far-from-equilibrium function, and decreases the reaction rate in a non-linear way as the solution approaches equilibrium. The extra subscript "actual" on the activity *a* in Equation (30) distinguishes the actual non-equilibrium activity for the equilibrium activity in Equation (31). The *c* in Equation (31), is either the concentration or mole-fractions, depending on the actual units used for the K-values. A similar consistent formulation will occur in Equation (30), for the real concentrations and corresponding activity coefficients *γ*, for actual non-equilibrium conditions. The term $acc_i^{p_i}$ accounts for the catalytic effect of some species (particularly of H+) and the value of p_i is determined by fitting experimental data. For reactions that are slow at ambient conditions, the experiments are carried out at temperatures that are sufficiently high to result in dissolution within reasonable reaction times. Scaling of the rate constants are normally done through the Arrhenius equation

$$k_m = k_0 \exp(\frac{-E_{a,m}}{RT}) \tag{32}$$

where k_0 is a constant and $E_{a,m}$ is the apparent activation energy of the overall reaction process that for most minerals range from 30 to 80 kJ/mol. The parameters k_0 and $E_{a,m}$ are determined from experiments performed at different temperatures.

2.3 The coupling of CodeBright and Retraso

The coupling of Retraso and CodeBright is described as follows: In one time step, which is pre-described by user, the CodeBright module first calculates the mass flow, heat transport and geomechanical deformation. All these properties, as well as physical properties and state conditions like liquid pressures (Pl), gas pressures (Pg), temperatures (T), deformations (u), flux of liquid, flux of gas, and hydraulic saturation, are transferred to Retraso. The initial integration time step defined in CodeBright, is divided into a smaller subdivision for integration over the fluxes of individual molecules and ions, taking into account possible reactions between fluids and solid, in either an equilibrium approximation or reaction kinetic formulation (Lasaga et al., 1984). Porosity is updated according to mineral erosion or mineral precipitation, and permeability is updated according to a commonly used correlation (Kozeny, 1927). All detailed results from the individual fluxes and phase properties are then transferred back to CodeBright for next time step. Both CodeBright and Retraso adopt the Newton-Raphson iterations to solve the non-linear algebraic systems of governing equations. Since extensive modifications of the original code are implemented through this project, the current algorithms will be described in sufficient detail below for future reference. The coupling of the two modules is schematically illustrated in Fig. 2.

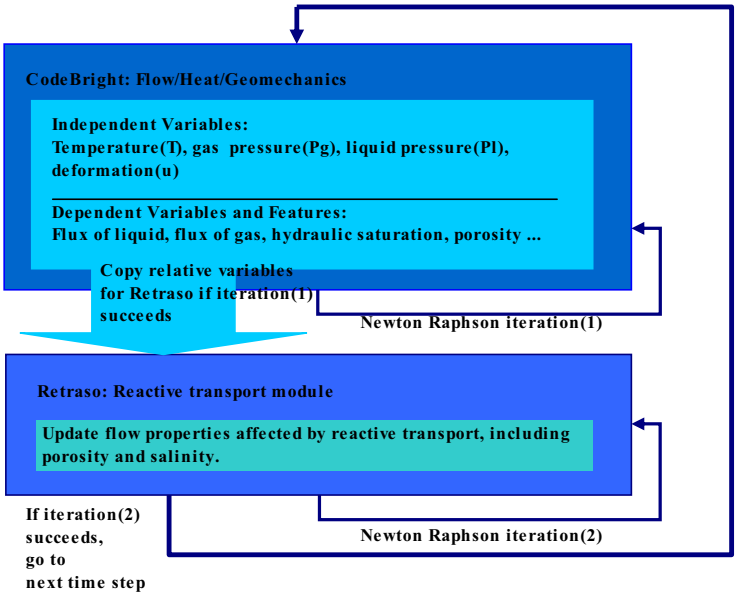

Fig. 2 RCB solves the integrated equations sequentially in one time step

2.4 The graphical user interfaces

The software VisualRetraso by Saaltink et al. (2005) and a software called GiD by the International Center For Numerical Methods In Engineering (CIMNE), are the two interactive graphical user interfaces, for pre- and post-processing, i.e., for the definition, preparation, and visualization, of all the data related to the numerical simulator RetrasoCodeBright. VisualRetraso reads all the data, including a definition of the geometry, the geochemical data, and the thermal-hydraulic-geomechanical data. The program then generates a mesh for finite-element analysis and output the information for RetrasoCodeBright in its desired format. Then the output information, together with the chemical equilibrium database and the kinetics database, are read by RetrasoCodeBright for numerical simulation. When the simulation finishes, the mesh with all the results are sent to GiD for visualization. Fig. 3 illustrates the whole workflow.

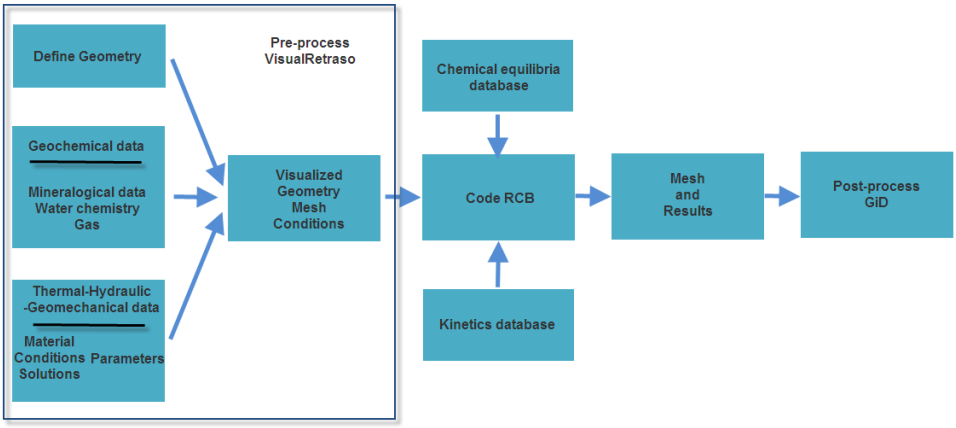

Fig. 3 The workflow of the pre-process VisualRetraso, code RCB and post-process GiD

3. Extended code RCB for coupled Thermo-Hydro-Mechanical-Chemical transport problems in CO_2 storage in saline aquifers modeling

As discussed in the introduction in Chapter 2, RCB is a numerical tool developed for coupled hydro-thermal-geomechanical-geochemical modelling. However, to be able to simulate CO_2-storage scenarios, RCB must be further extended. The extensions include an improvement of the Newton-Raphson scheme to strengthen the robustness of the numerical iterations in CodeBright and the possibility of specifying CO_2 gas properties in Retraso, i.e. the CO_2 gas-density correction and corrections on solubility of CO_2. These extensions will be introduced in Sections 3.1 and 3.2 respectively.

3.1 Improved Newton-Raphson iteration method in CodeBright module

The original RCB applies the ideal-gas assumptions, which is far from the state of the CO_2 that is injected and then migrates under high temperature and high pressure conditions in deep saline aquifers. The extension of a hydro-geological simulator from ideal-gas assumption into a high-pressure CO_2-storage simulator turned out to be far more challenging than just implementing corrections for densities and gas solubility. The numerical algorithms have been extensively rewritten in order to increase the convergence qualities of the code.

The governing equations for non-isothermal multiphase flow of liquid and gas, through porous deformable saline media, have been established. Variables and corresponding equations are listed in Table 1.

Equation	Variable name	Variable
Equilibrium of stresses	Displacements	u
Balance of liquid mass	Liquid pressure	Pl
Balance of gas mass	Gas pressure	Pg
Balance of internal energy	Temperature	T

Table 1 Equations and independent variables

After the spatial discretization of the partial differential equations, the residuals obtained can be written (for one finite element) as

$$\begin{pmatrix} r_u \\ r_{Pl} \\ r_{Pg} \\ r_T \end{pmatrix} = \frac{d}{dt}\begin{pmatrix} d_u \\ d_{Pl} \\ d_{Pg} \\ d_T \end{pmatrix} + \begin{pmatrix} a_u \\ a_{Pl} \\ a_{Pg} \\ a_T \end{pmatrix} + \begin{pmatrix} b_u \\ b_{Pl} \\ b_{Pg} \\ b_T \end{pmatrix} = \begin{pmatrix} 0 \\ 0 \\ 0 \\ 0 \end{pmatrix} \tag{33}$$

where **r** is the vector of residuals, $d\mathbf{d}/dt$ contains the storage or accumulation terms, **a** is the vector of conductance terms, and **b** contains the sink/source terms and boundary conditions. After discretization in time, a more compact form is

$$r\left(X^{k+1}\right) = \frac{d^{k+1} - d^k}{\Delta t^k} + A\left(X^{k+\varepsilon}\right)X^{k+\theta} + b\left(X^{k+\theta}\right) = 0 \tag{34}$$

where k is the time step index, : $\mathbf{X}=[(ux,uy,uz,Pl,Pg,T)_{(1)}, \ldots, (ux,uy,uz,Pl,Pg,T)_{(n)}]$, is the vector of unknowns (i.e. a maximum of six degrees of freedom per node), and **A** represents the conductance matrix. The Newton-Raphson scheme for solution of this non-linear system of AE's is

$$\frac{\partial r\left(X^{k+1}\right)}{\partial X^{k+1}}\left(X^{k+1,l+1}-X^{k+1,l}\right)=-R\left(X^{k+1,l}\right) \tag{35}$$

where *l* indicates iteration. In the present approach, the standard Galerkin method is used with some variations in order to facilitate computations.

The mathematical equations for the system are highly non-linear and they will be solved numerically. The numerical approach can be viewed as divided into a spatial and a temporal discretization. A finite element method is used for the spatial discretization while finite differences are used for the temporal discretization. The discretization in time is linear and the implicit scheme uses two intermediate points, $t^{k+\varepsilon}$ and $t^{k+\theta}$ between the initial t^{k} and final t^{k+1} times.

The Newton-Raphson method is adopted to derive the iterative scheme. This scheme is been modified through the introduction of a relaxation factor according to the algorithms of Nakata and Fujiwara (Nakata et al., 1993), in which we obtain the proper relaxation factors, denoted by α, combining the general-tendency method and time-step-reduction method.

The Newton-Raphson iteration scheme is rewritten as

$$X_{new}^{k+1,l+1}=X^{k+1,l}+\alpha\bullet(X^{k+1,l+1}-X^{k+1,l}) \tag{36}$$

where *l* is the iteration number, α is between 0 and 1, and α is not unique.

Commonly, if the relaxation factor that minimizes the total square residual for the Galerkin method, then this relaxation factor is introduced at each step of the nonlinear iteration, a convergent solution can be always obtained (Nakata et al., 1993). Therefore, we name the relaxation factor, the optimum relaxation factor, marked as α_m. However, usually it is computationally very expensive to determine it, because a large number of repeated square-residual calculations is required. Therefore, the time-step-reduction algorithm is adopted to iteratively find α_m. The algorithm always starts with a conventional Newton method with $\alpha=1$, and the value is reduced to half of the previous value, following

$$\alpha^{(k)} = 1/2^n \qquad (k = 1,2,...n = 0,1,2,...) \tag{37}$$

where k is the iteration number. Following each iteration the total square residual of the Galerkin method is calculated and compared with the previous value. The relaxation factor α^k is selected, when following criterion is satisfied,

$$\sum_{i=1}^{mu} \left\{ G_i^{k+1} \right\}^2 \le \sum_{i=1}^{mu} \left\{ G_i^{k} \right\}^2 \tag{38}$$

This robust method ensures, not only, that the optimal factor can be determined, but also, that it can be determined with a significantly less computational effort.

3.2 Estimation of CO_2 properties in code Retraso

The properties of carbon dioxide are important in the calculation of the rate of gas-flow through the reservoir rock, in material balance calculations, for evaluation of gas reserves, and in reservoir simulations. In the CO_2-storage scenarios, gas mixtures, including CO_2 gas and other non-CO_2 gases, are injected into the storage formations. The methods available in the literature, for the calculation of the properties of CO_2 gas, can be classified into three groups. The first group uses gas composition or gas gravity to calculate pseudo-critical properties of gases and predicts gas properties from empirical correlations. The second group uses gas composition to estimate gas properties via the method of corresponding states. The third group is based on the equations of state (EOS) approach and has the advantage of using a single equation to calculate the *k*-value, compressibility, density, and viscosity (Guo et al., 2001). The use of an EOS also ensures stable convergence in the vicinity of the critical point. Furthermore, in EOS-based viscosity models the density calculation is not required for computation of viscosity.

At the current stage the primary goal of this project is to demonstrate features of Retraso, and the Soave-Redlich-Kwong EOS (Soave, 1972) that is used to calculate the compressibility factor of CO_2 fluid, and details are presented in Sections 3.2.1 and

3.2.2. The corrected mass-balance equation for CO_2 reactive transport is presented in Section 3.2.3. Even though SRK-EOS is not the best equation for this purpose, corrections can be applied to improve the accuracy of this EOS for gas-property prediction. At the current stage the primary goal is to demonstrate the features of Retraso. The functions for thermodynamic and transport property calculations can be easily changed in the code at later stages later.

3.2.1 Gas density correction

The gas equation is written as

$$PV = ZnRT \tag{39}$$

where P is the pressure, V is the volume, Z is the compressibility factor for the gas, n is the number of moles, R is the ideal gas constant, and T is the temperature. The compressibility factor for CO_2 is calculated using the SRK-EOS tabulated as function of temperature T and pressure P, and estimated by bilinear interpolation (Hellevang and Kvamme, 2007).

The concentration of CO_2 in gas phase (c_{CO2}) is expressed in mole per unit of volume as

$$c_{CO2} = \frac{P}{ZRT} \tag{40}$$

The gas density of CO_2 is:

$$\rho_{CO2} = \frac{PM_{CO2}}{ZRT} \tag{41}$$

where M_{CO2} is the molar weight of CO_2 (44.01 g/mol), R is the gas constant (8.3143 $J \cdot K^{-1} \cdot mol^{-1}$). The units of P and T, are respectively in bar and Kelvin.

3.2.2 Correction on CO_2 solubility

The bubble-point mole fraction of CO_2 is calculated according to

$$x_{CO2}^{b} = \frac{P\varphi}{H_{CO2}} \exp\left\{ \frac{\bar{v}^{\infty}}{RT}(1-P) \right\} \tag{42}$$

where φ is the fugacity coefficient for CO_2 estimated from the SRK-EOS, H_{CO2} is the Henrys-law coefficient for CO_2, P is pressure (bar), T is temperature (K), R is the gas constant, and v^{∞} is the partial molar volume of CO_2 at infinite dilution. The fugacity coefficient is calculated as a function of temperature and pressure by a polynomial that is interpolated from SRK data. The Henrys-law coefficient is found from a polynomial that is interpolated as a function of temperature and salinity from listed experimental data (Zheng et al., 1997). Finally, x_{CO2}^{b} is the Poynting correction to the Henrys-law coefficient.

3.2.3 mass balance equation for CO_2 reactive transport

The chemistry of CO_2-gaseous species is added to the reactive transport equation, which becomes

$$U_a \frac{\partial \phi S_l \rho_l c_a}{\partial t} + U_m \frac{\partial (1-\phi)\rho_s c_m}{\partial t} + U_g \frac{\partial \frac{\phi S_g}{Z_{co_2} RT} P_{co_2}}{\partial t} = U_a L_l(c_a) + U_g L_g(P_{co_2}) + U S_k^t r_m(c_a) \tag{43}$$

This equation constitutes the Nc reactive-transport equations, where Nc means the numbers of primary species in the system. Vectors c_a , c_m (mol kg^{-1}) are the concentrations of aqueous species, and mineral species, and P_{co_2} is the partial pressure of CO_2. The matrices U_a, U_m, and U_g, are named the component matrices for aqueous, mineral, and gaseous species, and the matrices relate the concentrations of the species to the total concentrations of the components. The variable ϕ is the porosity of the media, while S_l and S_g are respectively the liquid and gas

saturation, R is the gas constant, T is the temperature, and Z_{co_2} is the compressibility factor for CO_2. The matrix U is the component matrix for all the species. Together with U_a, U_m, and U_g, all these matrices can be calculated from the stoichiometric coefficient of the chemical reactions. The matrix S_k and vector r_k contains the stoichiometric coefficients and the rates of the kinetic reactions, which can be considered as functions of all aqueous concentrations. We have also defined L_l and L_g as linear operators for the advection and dispersion/diffusion as

$$L_l() = -\nabla \bullet (q_l \rho_l()) + \nabla \bullet (D_l \phi S_l \rho_l \nabla()) + m_l \tag{44}$$

$$L_g() = -\nabla \bullet (q_g \frac{1}{Z_i R T}()) + \nabla \bullet (D_g \phi S_g \nabla \frac{()}{Z_i R T}) + m_g \tag{45}$$

where m_l and m_g are the non-chemical source-sink terms (mol m^{-3} s^{-1}) and D_l and D_g are the dispersion/diffusion tensors (m^2 s^{-1}), for the liquid and gas phase. Finally, Z_i is the compressibility factor for ith gas.

4. Two examples for demonstrating geomechanical effects of CO_2 injection in cold aquifers with possibility of hydrate formation and sandstone

Two 2D hydro-chemical-mechanical models are presented in this section. Both of the two models are created which have 3 layers (2 layers with aquifers and 1 layer with cap rock on which two fractures are introduced). The differences between these two models are most on temperature. In the first example where the formation temperature is low and hydrate formation possibility is included in the model. The temperature in the second example is relatively high and the conditions in the example below are outside hydrate stability region. RetrasoCodeBright has been used to simulate the storage of CO_2 in this model. For this purpose hydrate has been added as a pseudo-mineral component and the hydrate phase transition dynamics have been implemented into RetrasoCodeBright along with kinetic description of ordinary mineral/fluid reaction kinetic models. Corrections for effects of porosity changes on permeability are included but so far based on traditional correlations for mineral/fluid. We focus on the implications of the dissociation or precipitation of minerals as well as hydrate formation or dissociation (according to the value of pH) on geomechanical properties of the reservoir (Kvamme B. et al., 2011).

4.1 CO_2 injection in cold aquifers with the possibility of hydrate formation

We study the hydro-mechanical changes associated with CO_2-injection into a brine formation. The geometry of the 2D domain is 1000m x 250m rectangle. There are 2 aquifers, 3 cap rocks and 2 fracture zones in the geometry. The area in the bottom and top are aquifers. Bottom aquifer is a 1000m x 150m rectangle and top aquifer is 1000m x 50m rectangle. The three zones between two aquifers are cap rocks with dimension of 298m x 50m in both sides and 396m x 50m in the middle. There are two fracture zones, one between left and middle side cap rocks, the other between

middle and right side cap rocks. These fractures have dimensions 4m x 50m each. CO_2 is injected at 50 meter height from the bottom in the bottom aquifer as shown in the Fig. 4.

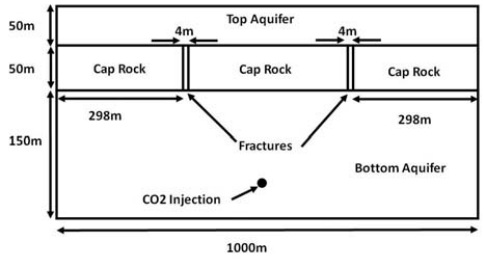

Fig. 4 Schematic of the model

Composition of rocks in each zone is as follows; aquifers have a porosity of 0.1 and among minerals it has 10% calcite, 80% quartz. Pressure and temperature at each node are defined in one of the input files. In reservoir pressure gradient is 1.0 MPa/100m and temperature gradient is 3.6 °C/100m. CO_2 injection pressure is 4.6 MPa. Pressure boundaries are also defined at top and bottom of the reservoir, at the top 2.5 MPa and at the bottom 5 MPa. Pressure boundaries enclose the reservoir. The initial stresses are given in absolute values in a range from 5.67 MPa on upper boundary to 11 MPa on the bottom boundary. The initial temperature at the upper boundary is 4°C and 11.2°C at the bottom. The summary of this model and properties are presented in Table 2 to 6.

Aquifers	Cap rock and fractures
Ca+2	Ca+2
H2O	H2O
HCO3-	HCO3-
H+	H+
SiO2(aq)	SiO2(aq)
CaCO3(aq)	CaCO3(aq)
CaH2SiO4(aq)	CaH2SiO4(aq)
CaHCO3+	CaHCO3+
CaOH+	CaOH+
CO_2(aq)	CO_2(aq)
CO3-2	CO3-2
OH-	OH-
H2SiO4-2	H2SiO4-2
HSiO3-	HSiO3-

Table 2 chemical species (primary and secondary aqueous species) in different formations

	Mineral volume fraction with 11.1% calcite [m3/m3]	**Mineral reactive surface with 11.1% calcite, [m2/m3]**
Aquifers; 10% porosity	Calcite (0.1) Quartz (0.8)	Calcite (100) Quartz (800)
Cap rock; 1% porosity	Calcite (0.1) Quartz (0.89)	Calcite (100) Quartz (890)
Fractures; **5% porosity**	Calcite (0.1) Quartz (0.85)	Calcite (100) Quartz (850)

Table 3 Initial composition of minerals

Zone	**Aquifers**	**Cap rocks**	**Fractures**
Permeability (m^2)	1e-13	1e-17	1e-12
Longitude dispersion factor (*m*)	11	11	11
Molecular diffusion (*m*)	1e-10	1e-10	1e-10

Table 4 Permeability, dispersion and molecular diffusion

Property	Aquifers	Cap rocks	Fractures
Young's modulus, E [GPa]	0.3	0.3	0.3
Poisson's ratio	0.2	0.2	0.2
Porosity	0.1	0.01	0.05
Zero stress porosity, Φ_0	0.1	0.01	0.05
Zero stress permeability, K_0 [m2]	1.0e-13	1.0e-17	1.0e-12
Irreducible gas and liquid saturation, S_{rg}	0	0	0
Van Genuchten's gas-entry pressure, P_0 [MPa], (at zero stress)	0.0196	0.196	0.196
Van Genuchten's exponent [m]	0.457	0.457	0.457

Table 5 Material properties

Parameter	Bottom Boundary	Top Boundary
Pressure, P(MPa)	5	2.5
Mean Stress, σ(MPa)	11	5.67
CO_2 **initial injection pressure, P_g (MPa)**	4.6*	-
CO_2 **final injection pressure, P_g (MPa)**	4.6*	-
Gas and liquid outgoing pressure (MPa)	5	2.5
Temperature(°C)	11.2	4

* at the injection point

Table 6 Initial and boundary conditions

Simulation results for different time steps are presented in the following. Liquid and gas phase fluxes, porosity and effective stress are the parameters of interest. Each figure shows the results at three time steps: results for starting day at the top, after 280 days at the middle and results after 563 days at the bottom, which for effective stress figure it is 320 days.

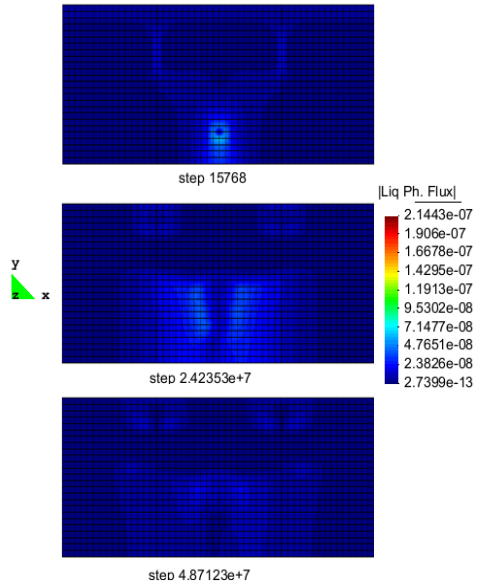

Fig. 5 Liquid phase flux (m/s) at starting day (top), after 280 days (middle) and 563 days

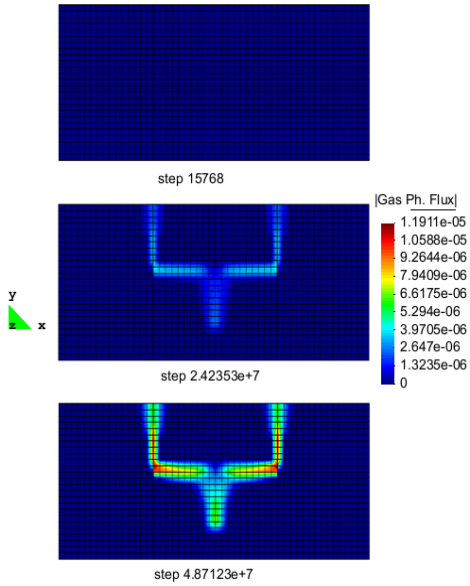

Fig. 6 Gas phase flux (m/s) at starting day (top), after 280 days (middle) and 563 days

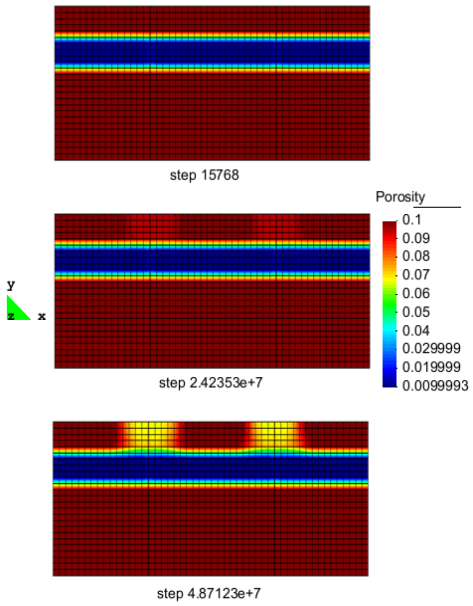

Fig. 7 Porosity changes at starting day (top), after 280 days (middle) and 563 days

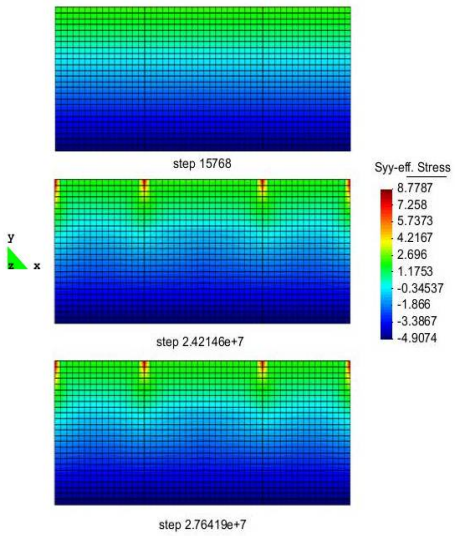

Fig. 8 Effective stress at starting day (top), after 280 days (middle) and 320 days

Figure 5 and 6 show the liquid and gas phase fluxes respectively. These figures clearly show that because of the fractures flow will reach the upper aquifer in a

relatively short time. As soon as CO_2 reaches the top aquifer, it will start forming hydrate due to suitable temperature and pressure conditions as shown in figure 7. Figure 8 shows the effective stress in yy direction in the reservoir. According to this figure, minimum effective stress is -4.9074 MPa. A comparison between tensile strength of sand stone is in the literature (Huang S. et al, 2010) and the minimum effective stress in this simulation suggests that it might be in the range of tensile strength for similar material.

4.2 CO_2 injection in sandstone

The geometry of the second model has 2D domain which is 1000m x 500m rectangle. There are 2 aquifers, 3 cap rocks and 2 fracture zones in the geometry. The area in the bottom and top are aquifers. Bottom aquifer and top aquifer are 1000m x 200m rectangular. The three zones between two aquifers are cap rocks with dimension of 300m x 100m in both sides and 392m x 100m in the middle. There are two fracture zones, one between left and middle side cap rocks, the other between middle and right side cap rocks. These fractures have dimensions 4m x 100m each. CO_2 is injected at 30 meter height from the bottom in the bottom aquifer as shown in the Fig. 8.

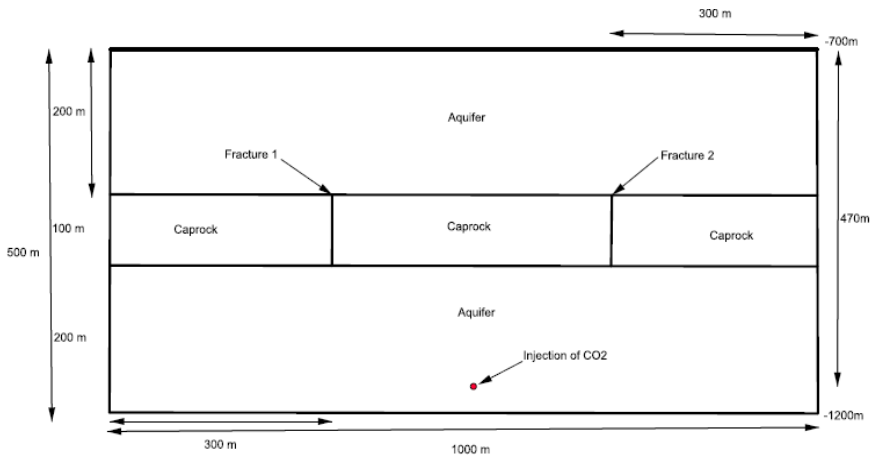

Fig. 8 Schematic of the model

Composition of rocks in each zone is as follows; aquifers have a porosity of 0.1 and among minerals it has 4% calcite. Pressure and temperature at each node are defined in one of the input files. In reservoir pressure gradient is 1.0 MPa/100m and temperature gradient is 3.6 °C/100m. CO_2 injection pressure is 14.5 MPa. Pressure boundaries are also defined at top and bottom of the reservoir, at the top 10 MPa and at the bottom 15 MPa. Pressure boundaries enclose the reservoir. The initial stresses are given in absolute values in a range from 22.28 MPa on upper boundary to 33.14 MPa on the bottom boundary. The initial temperature is 36°C at the top and 54°C at the bottom. The summary of this model and properties are presented in Table 7 to 10.

Property	Aquifers	Cap rocks	Fractures
Young's modulus, E [GPa]	0.5	0.5	0.25
Poisson's ratio	0.2 5	0.2 5	0.2 5
Porosity	0.1	0.01	0.05
Zero stress porosity, Φ_0	0.1	0.01	0.05
Zero stress permeability, k_0 [m^2]	1.0e-13	1.0e-17	1.0e-12
Irreducible gas and liquid saturation, S_{rg}	0	0	0
Van Genuchten's gas-entry pressure, P_0 [MPa], (at zero stress)	0.0196	0.196	0.196
Van Genuchten's exponent [m]	0.457	0.457	0.457

Table 7 Material properties

Species	Aquifers: 10% porosity	Cap rock: 1% porosity	Fractures: 5% porosity
Mineral volume fraction with 4% calcite [m3/m3]	Calcite (0.036) Quartz (0.864)	Calcite (0.04) Quartz (0.95)	Calcite (0.038) Quartz (0.912)
Mineral reactive surface with 4% calcite, [m2/m3]	Calcite (36) Quartz (864)	Calcite (40) Quartz (950)	Calcite (38) Quartz (912)

Table 8 Initial composition of minerals

Parameter	Bottom Boundary	Top Boundary
Pressure, (MPa)	15	10
Mean Stress, (MPa)	33.14	22.28
Temperature (°C)	54	36
CO_2 **initial injection pressure, (MPa)**	14.5 (at the injection point)	-
CO_2 **final injection pressure, (MPa)**	14.7 (at the injection point)	-
Gas and liquid outgoing pressure (MPa)	15	10

Table 9 Initial and boundary conditions

Zone	Aquifers	Cap rocks	Fractures
Permeability (m^2)	1e-13	1e-17	1e-12
Longitude dispersion factor (*m*)	11	11	11
Molecular diffusion (*m*)	1e-10	1e-10	1e-10

Table 10 Permeability, dispersion and molecular diffusion

Simulation results for different time steps are presented in the following. Gas phase fluxes, effective stress, liquid pressure, gas pressure and liquid saturation are the parameters of interest. Each figure shows the results at two time steps: results after 12 months at the top and results after 27 months at the bottom.

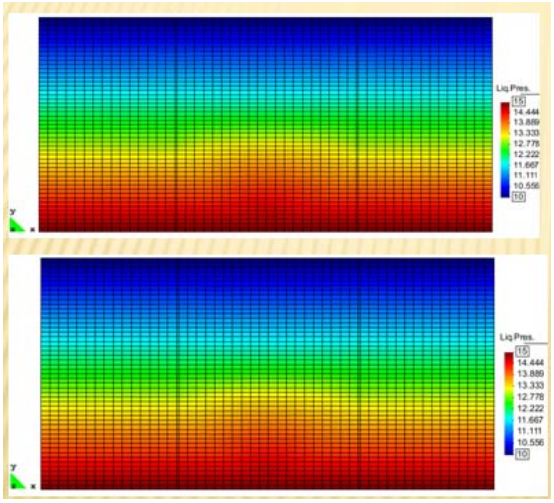

Fig 9 Liquid pressure after 12 months and 27 months

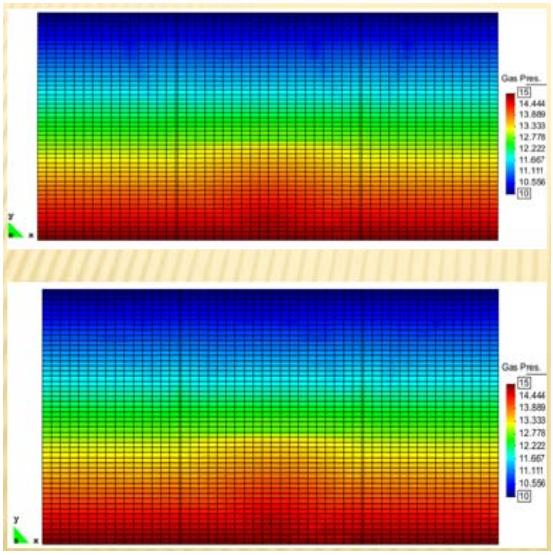

Fig 10 Gas pressure after 12 months and 27 months

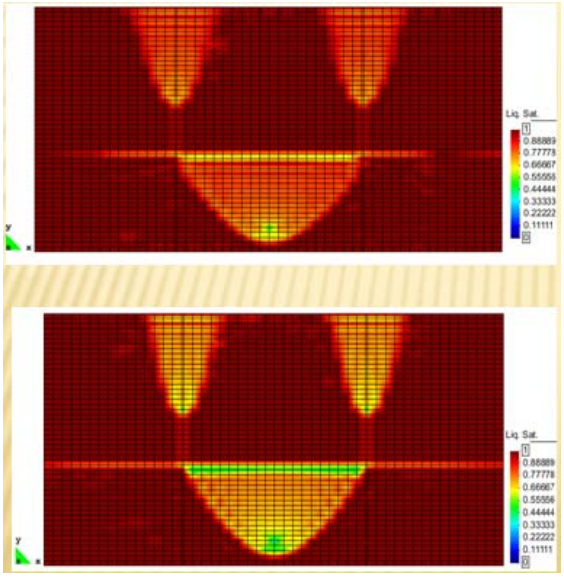

Fig 11 Liquid saturation after 12 months and 27 months

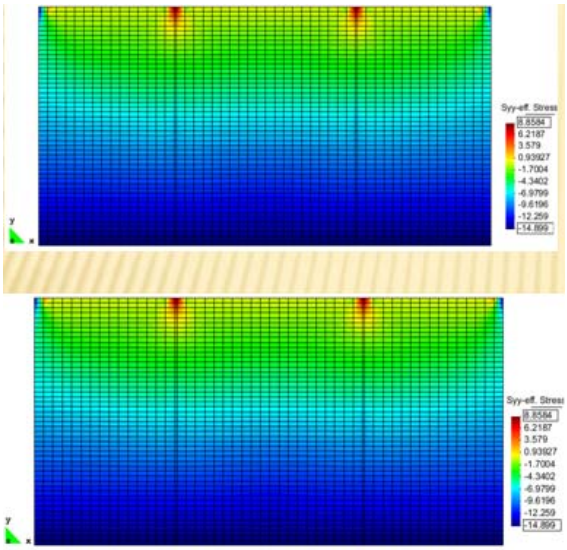

Fig 12 Effective stress in “yy” direction after 12 months and 27 months

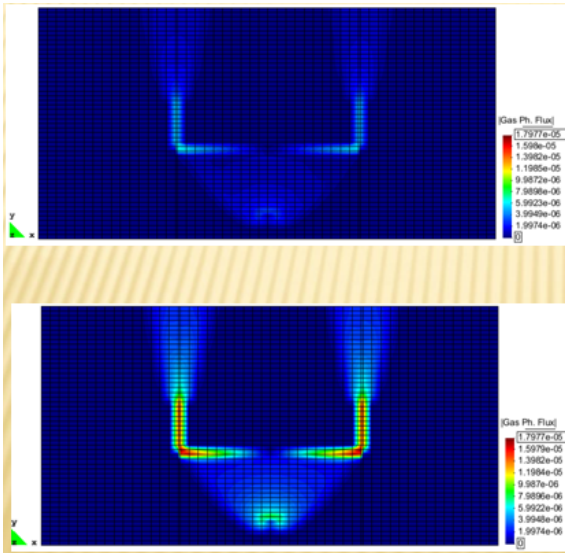

Fig 13 Gas phase flux (m/s) after 12 months and 27 months

5. Introduction to the papers

The main part of this thesis consists of a collection of published papers concerning modelling of CO_2 storage in saline aquifers by using the simulator RetrasoCodeBright.

Paper1 has introduced the extended version of a geomechanical reactive transport simulator RetrasoCodeBright which can handle high pressures relevant for reservoir storage of CO_2. Corrections for non-ideal gas have been based upon the SRK equation of state which can be easily replaced by similar results from any equation of state since the necessary data are interpolated from calculated tables of compressibility factors and fugacity as function of temperature and pressure. The convergence of the Newton-Raphson iterative solution has been improved through implementation of an algorithm that minimizes the total square residual from the Galerkin method after each iteration step. The corrected version has been applied to a simple test case where the reservoir only has aquifers without any cap rock sealing.

Paper2 has also introduced the new CO_2 storage simulator on the RetrasoCodeBright platform by inclusion of non-ideal gas description using an equation of state for calculation of gas solubility and incorporation of realistic fluid densities as function of local pressure and temperature. A test case has been used to illustrate numerical solution from the new CO_2 simulator. In this case the geological size of the reservoir has been enlarged and a cap rock layer has been put on the top of aquifer.

Paper3 is a chapter of book “Carbon Dioxide Capture for Storage in Deep Geological Formation”, volume 3. This book is a summary of results from the Carbon Capture Project stage 2 (CCP2) which was a Joint Industrial Program headed by Chevron and BP. In this paper we have reported the motivation of developing a CO_2 storage simulator which is able to address geochemical and geomechanical reservoir stability concerns within one implicit software package. All the equations in the original code RetrasoCodeBright and the extensions which haven been made into this code have

been introduced in detail. Two 2D hydro-chemical-mechanical problems are used to illustrate the modified RCB code. The purpose of the first case is to demonstrate implications of geochemical buffering in systems containing high portions of rapidly dissolving calcite, while the second test case gives examples of fracture description using the classical approach of defining a fracture through extremely high permeability.

Paper4 focus on explaining the improved Newton-Raphson iteration method which has been included in code RetrasoCodeBright. The traditional Newton-Raphson method can tend to diverge due to a number of causes. Reactive flow simulations in porous medium with implicit geomechanical analysis are very complex problems which require more robust iteration method. By adding an optimum relaxation factor the solutions of the equations can be successfully found even when the conditions are extreme.

Paper5 focus on the importance of geomechanical implications of the changes on the stability of the reservoir in the evaluation of potential injection reservoirs. In cold aquifers the formation of CO_2 hydrate will affect flow paths and may also have implications on the geomechanical stability due to the increase in volume of the formed hydrate. In this paper a 2D hydro-chemical-mechanical problem is solved by the improved RCB code. The results are presented and compared. Strategies for using the simulator for hydrate exploitation purposes have also been discussed.

Paper6 has given a detailed introduction on the current on-going geological CO_2 storage projects worldwide, of which two are the Sleipner and Snøhvit projects in Norway. The Slepner project has been running since 1996. One million tones of CO_2 are captured and stored in a sandstone formation Utsira. The Snøhvit project is located in the Barents Sea. It started in October 2007 and more than 700,000 tones of CO_2 are stored yearly. In Algeria a CO_2 sequestration project in connection with In Salah Gas has started in 2004. The injection volume is expected to reach 1.2 million tones per year. The IEA Weyburn project intends to demonstrate that CO_2-EOR is economically viable.

Paper7 focus on the importance of geomechanical stability to CO_2 sequestration and pointed out the advanced implicit geomechanical coupling in the CO_2 storage simulator RetrasoCodeBright. A literature survey of alternative current codes for CO_2 storage modelling has been conducted in this paper, revealing that different models have different interpretation of the given conditions by different assumptions and simplifications and strong differences in their numerical performance. In particular the importance of an implicit algorithm for geo mechanics is stressed. Some chemical reactions with minerals under low pH are fast and in addition some storage reservoirs offshore Norway may contain regions of hydrate formation - which is orders of magnitude faster. An implicit algorithm for geomechanics is therefore highly recommended to ensure that dynamic information is not lost between the flow evaluation and a time shifted evaluation of the geomechanics. A test case with aquifer, cap rock and a fracture has been setup in this paper. By varying the initial composition of minerals, sensitivity test has been carried out on the test case.

6. Proposed future work

Non-isothermal effect

In the RCB code, the internal-energy-balance equations constitute an important part of the computational tool, and are used to model the three main processes of energy transfer, i.e. heat conduction, advection of heat (due to mass flux), and phase changes. Evaluations of the code so far have not considered temperature changes since emphasis have been on increasing the numerical stability of the simulator and implementation of more critical aspects of non-ideal gas (solubility, gas density). For further use of the code there are some phenomena which depend sensitively on temperature, in particular the potential of degassing of dissolved CO_2 from the aqueous solution at high temperatures deeper in the reservoir. Non-polar or slightly polar gas phase (CO_2) is a thermal insulator but higher density will still make a difference from ideal gas. Enthalpy changes of CO_2 can be derived directly from the same equation of state which is used for other properties or alternative correlations which may be more accurate. Some experimental data as well as correlations for efficient heat conductivity (also taking into account some impact of heat convection) is available in the open literature but have not been evaluated at this point. Implementation should be fairly straightforward.

Geochemical data

The mineralogical composition of the Utsira formation consists of mainly of quartz, K-feldspars, plagioclase, mica, and calcite (Pearce et al. 1999). Dissolution of original minerals in low pH zone (close to injection) and transport of ions with flow to regions of higher pH leads to precipitation of same type of minerals as well as other secondary minerals like for instance magnesite, dawsonite, and gypsum. At the current stage of the simplified examples we have not considered all possible precipitation minerals although there are some new available kinetic data on minerals like for instance dawsonite which might shed light on possible precipitation effects in reservoirs like Utsira. dawsonite can benefit from aluminium dissolved from silicates

and sodium from groundwater so it would be interesting to evaluate the potential impact and stability of dawsonite precipitation at Utsira

Hydrodynamic fracture description

An important extension of the code would be the inclusion of a hydrodynamic description of flow through fractures and faults as hydrodynamic conduits described by Navier-Stokes equation, and with velocities between the conduit and the reservoir flow (Darcy flow) as the boundaries between the two different flow regimes. This hydrodynamic fracture description will also open up for realistic description of injection wells rather than treating these as point sources.

Relative permeability hysteresis

Unlike many other academic codes, RCB has built-in capabilities of changing permeability and relative permeability, in every time step. In the current version, permeability is updated as function of porosities that change due to mineral dissolution or mineral precipitation. As such, it should be possible to include relative-permeability hysteresis effects. The built-in adsorption facility will also enable a more realistic description of surface reactions as well as wetting preference characteristics of different minerals on residual pore saturations.

Hydrate sealing effects

Some relevant reservoirs for storage of CO_2 are located in regions of low seafloor temperatures and at depths that facilitates the formation of hydrate (ice-like solid with up to 12 mole percent CO_2) between CO_2 and water. These hydrates do not close the pore space since they are unable to attach to mineral surfaces due to hydrogen-bonding limitations. I.e., the partial charges on the surfaces of minerals are not compatible with the hydrogen bonded structure on the surfaces of hydrates. Thermodynamics will therefore induce a necessary bridging of more or less structured water, separating the hydrates from the mineral surfaces. The thickness of a minimum bridging layer corresponds to 4 - 6 water layers (or in the order of 2 nm), which may practically reduce the permeability to a very low level, and it may as such

provide more time for the CO_2 plume to dissolve into the surrounding groundwater and sink. As such, the extra sealing achieved may actually promote the search for storage reservoirs in which hydrates may form. Within RCB, this sealing process can be treated as a pseudo mineral reaction in which hydrates form at the CO_2-water interface and then the hydrates may dissolve again in water with lower concentration of CO_2. This dynamic process is often controlled by mass transport, as investigated and published in several papers from the group led by Professor Bjørn Kvamme. Another reason for implementing hydrate sealing effects is to capture the dynamics of the formation (roughly 10% volume increase compared to liquid water) and dissociation and the potential geomechanical impact on the geological structure. The further implementation of hydrate sealing effects is a future research area that should be given high priority. Offshore Norway, Utsira is too warm for hydrate formation while Snøhvit injection is cold enough in the upper section if the CO_2 plume reaches the upper layers. The injection location on Snøhvit is very deep, and due to the lack of openly available data on the formation, it has so far not been possible to simulate possible migration patterns for the injected CO_2.

7. References

Alonso E. E., Gens A., and Josa A., "A constitutive model for partially saturated soils", *Géotechnique,* 1990, vol. 40, no. 3, pp. 405-430.

Alonso E. E. Olivella, S. and N. M. Pinyol, "A review of Beliche Dam", *Géotechnique,* 2005, vol. 55, no. 4, pp. 267-285.

Bear, J. and Y. Bachmat, "Macroscopic Modelling of Transport Phenomena in Porous Media. 2: Application to Mass, Momentum and Energy Transport", *Transport in Porous Media 1*, 1986, pp. 241-269.

Bouc, O., Audigane P., Bellenfant, G., Fabriol, H., Gastine, M., Rohmer, J., Seyedi, D., "Determining safety criteria for CO_2 geological storage", Energy Procedia, 1, 1, 2009, Proceedings of the 9th international Conference on Greenhouse Gas Control Technologies, pp. 2439-2446.

Celia, M.A, Nordbotten, J.M., Bachu, S., Kavetski, D. and Gasda S., "Summary of Princeton Workshop on Geological Storage of CO_2", Princeton University, 1-3 November, 2005.

Colmenares, L.B. and M.D. Zoback, "A statistical evaluation of intact rock failure criteria constrained by polyaxial test data for five different rocks", *Int J Rock Mech Min Sci* 39:695-729, 2002.

Drucker, D.C. and Prager, W., "Soil mechanics and plastic analysis for limit design", *Quarterly of Applied Mathematics*, vol. 10, no. 2, 1952, pp. 157-165.

Ennis-King, J. and Paterson, L., "Role of Convective Mixing in the Long-Term Storage of Carbon Dioxide in Deep Saline Formations", paper SPE 84344 presented at the SPE Annual Technical Conference and Exhibition, 5-8 October 2003, Denver, Colorado.

Erdogmus, M., M.A. Adewumi, S.O. Ibraheem, "Viscosity Prediction of Natrual Gases", SPE 39219, Proceedings of the presentation at the Eastern Regional Meeting, Lexington, Kentucky, 22nd-24th October 1997.

Evans, J.P. *et al.*, "Natural Leaking CO_2-charged Systems as Analogs for Geologic Sequestration Sites", *Carbon Dioxide Capture for Storage in Deep Geologic Formations*; Results from the CO_2 Capture Project, Vol. 2, Elsevier Science, 2005, pp. 699-712.

Franklin M. Orr Jr., "Storage of Carbon Dioxide in Geologic Formations", *Journal of Petroleum Technology*, Vol. 56, No. 3, 2004, pp. 90-97.

Foxall, W. and Friedmann, S.J., "Frequently Asked Questions about Carbon Sequestration and Earthquakes", *LLNL-BR-408445*, 2008.

Gale, J., "Geological Storage of CO_2: What's Known, Where Are the Gaps, and What More Needs to Be Done", *Energy*, Vol. 29, Iss. 9-10, 2004, pp. 1329-1338.

Garitte, B. Vaunat, J. and A. Gens, "Thermo-Hydro-Mechanical Design Calculations for the TED Experiment", Internal Report for ANDRA (France), Department of Geotechnical Engineering and Geosciences, 2008.

Glass, H. *et al.*, "A benchmark study on problems related to CO_2 storage in geologic formations", Compute Geosci, 2009, DOI 10.1007.

Graue, A. and Kvamme, B., "Magnetic Resonance Imaging of Methane --- Carbon Dioxide Hydrate Reactions in Sandstone Pores", presented at SPE Annual Technical Conference and Exhibition, Texas, USA, 24th-27th September 2006.

Guo, X.Q., I.S. Wang, S.X. Rong, T.M. Guo, Fluid Phase Equilibria 139 (1977) 405-421.

Guo, X.Q., C.Y. Sun, S.X. Rong, G.J. Chen, T.M. Guo, J. Petrol. Sci. Eng. 30 (2001) 15-27.

Hambley, D.F., C.J. Fordham and P.E. Senseny, “General failure criteria for saltrock”, Rock Mechanics as a Guide for Efficient Utilization of Natural Resources, *Khair (ed.)* 1989, Balkema: pp. 91-98.

Harrington, J.F., and S.T. Horseman, “Gas Migration in KBS-3 Buffer Bentonite: Sensitivity of Test Parameters to Experimental Boundary Conditions”, SKB Technical Report TR-03–02, 2003.

Hawkes, C.D., McLellan, P.J., Bachu, S., “Geomechanical factors affecting geological storage of CO_2 in depleted oil and gas reservoirs”, *J. Can. Pet. Technol.* 44, 2005, pp. 52-61.

Hellevang, H., Kvamme, B., “An explicit and efficient algorithm to solve kinetically constrained CO_2-water-rock interactions”, *WSEAS TRANSACTIONS on Mathematics, 6, issue 5*, 2007, pp. 681-687.

Hoffert, M.I. *et al.*, “Advanced Technology Paths to Global Climate Stability: Energy for a Greenhouse Planet”, *Science* 298, 2002, pp. 981-987.

Holloway, S., “Safety of the underground disposal of carbon dioxide”, *Energy Conversion and Management*, vol. 38, pp. 241-245.

Holt, T.J., Lindeberg, E.G.B., and Taber, J.J., “Technologies and Possibilities for Large-Scale CO_2 Separation and Underground Storage”, paper SPE 63103 presented at the SPE Annual Technical Conference and Exhibition, 1-4 October 2000, Dallas, Texas.

Huang S., Xia K., Yan F and Feng X., “An experimental study of the rate dependence of tensile strength softening of Longyou Sandstone”, *Rock mechanics and rock engineering,* 2010, 43, pp 677-683.

Hunsche, U. and H. Albrecht, “Results of true triaxial strength tests on rock salt“, *Engineering Fracture Mechanics*, vol. 35, no. 4/5, 1990, pp. 867-877.

International Center For Numerical Methods In Engineering (CIMNE), "GiD reference manual, Pre and post processing system for F.E.M. calculations", International Center For Numerical Methods In Engineering (CIMNE), 2006.

Itasca Consulting Group Inc., "FLAC-3D Manual: Fast Lagrangian Analysis of Continua in 3 Dimensions Version 2.0", Itasca Consulting Group Inc., Minnesota, USA, 1997.

Izgec, O., and Demiral, B., "CO_2 Injection in Carbonates", Paper SPE 93773 presented at SPE Western Regional Meeting, Irvine, California, 30th March – 01st April, 2005.

Jaeger, J.C., Cook, N.G.W., "Fundamentals of Rock Mechanics", Methuen & Co. Ltd, 1969, London, UK.

Johnson, J.W. and Nitao, J.J., "Reactive Transport Modeling of Geologic CO_2 Sequestration at Sleipner", *Greenhouse Gas Control Technologies*, Vol. I, J. Gale and Y. Kaya (eds.), Elsevier, Amsterdam, 2003, pp. 327-332.

Juanes, R., C.W. MacMinn, and M.L. Szulczewski, "The Footprint of the CO_2 Plume during Carbon Dioxide Storage in Saline Aquifers: Storage Efficiency for Capillary Trapping and the Basin Scale", *Transport in Porous Media*, 2009, pp. 1573-1634.

Juvinal, Robert C. and Marshek, Kurt, "Fundamentals of machine component design", -2nd ed., 1991, pp. 217, ISBN 0-471-62281-8.

Kozeny, J., "Ube kapillar Leitug der Wasser in Boden, Sitzungsber", *Akad. Wiss. Wien*, 136, 1927, pp. 271-306.

Kumar, A. *et al.*, "Reservoir Simulation of CO_2 Storage in Deep Saline Aquifers", *SPE Journal*, Vol. 10, No. 3, 2005, pp. 336-348.

Kvamme, B., Graue, A.,Aspenes, E., Kuznetsova, T., Gránásy, L., Tóth, G., Pusztai, T.,Tegze G., "Towards understanding the kinetics of hydrate formation: Phase field

theory of hydrate nucleation and magnetic resonance imaging", *Physical Chemistry*, 2004, **6**, 2327 – 2334.

Kvamme, B., Graue, A., Kuznetsova, T., Buanes, T., Ersland, G., "Storage of CO_2 in natural gas hydrate reservoirs and the effect of hydrate as an extra sealing in cold aquifers", *International Journal of Greenhouse Gas Control*, 2007, Vol 1/2, pp 236-246.

Kvamme, B., Jemai, K., Chejara, A. and Vafaei T., "Simulation of geomechanical effects of CO_2 injection in cold aquifers with possibility of hydrate formation", Proceedings of the 7th International Conference on Gas Hydrates (ICGH), 2011, Edinburgh, Scotland, UK.

Lasaga, A.C., "Chemical kinetics of water-rock interactions", *Journal of Geophysical Research*, B6, 1984, pp. 4009-4025.

Lawal, A.S., "Prediction of Vapor and Liquid viscosities From the Lawal-Lake-Silberberg Equation of State", proceedings of the presentation at the SPE/DOE Fifth symposium on Enhanced Oil Recovery, Tulsa, OK, 20th-23rd April, 1986, paper SPE 14926.

Nakata, T. and Fujiwara, K., "Method for determining relaxation factor for modified Newton-Raphson method", *IEEE TANSACTIONS ON MEGNETICS*, vol. 29, No 2, 1993.

Olivella, S., A. Gens, J. Carrera, E.E. Alonso, "Numerical Formulation for a Simulator (CODE_BRIGHT) for the Coupled Analysis of Saline Media", *Engineering Computations*, vol. 13, No.7, 1996, pp. 87-112

Olivella, S., "Nonisothermal multiphase flow of brine and gas through saline media", doctoral thesis, 1995

Olivella, S., A. Gens, J. Carrera, E.E. Alonso, "Numerical Formulation for a Simulator (CODE_BRIGHT) for the Coupled Analysis of Saline Media", *Engineering Computations*, vol. 13, No.7, 1996, pp. 87-112.

Olivella, S. and E. E. Alonso, "Modeling the hydro-mechanical behaviour of GMT in situ test including interface elements", GMT Report, UPC-NAGRA, 2004.

Olivella, S. and A. Gens, "Double structure THM analysis of a heating test in a fractured tuff incorporating intrinsic permeability variations", *Int. J. Numer. Anal. Met. Geomech*. 42, 2005, pp. 667–669.

Olivella, S., Vaunat J., Garitte, B., and Pinyol, N.M., "Coupled THM problems in geotechnical engineering using CODE_BRIGHT-GiD", presented at 4rd GiD Conference, Ibiza, 2008.

Orlic, B., "Assessing the Mechanical Impact of CO_2 Injection on Faults and Seals", *CCS and Nuclear Waste Disposal, Fault and Top Seals: from Pore to Basin Scale,* 2009.

Parson, E.A. and Keith, D.W., "Fossil Fuels Without CO_2 Emissions", *Science* 282, 1998, pp. 1053-1054.

Patel, N., Teja, A., Chem. Eng. Sci. 37 (3), 1982, PP 463-473.

Pearce, J.M., Holloway, S., Wacker, H., Nelis, M.K., Rochelle, C., Bateman, K., "Natural occurrences as analogues for the geological disposal of carbon dioxide", *Energy Conversion and Management,*.37 (6-8), 1996, pp. 1123-1128.

Peng, D., Robinson, D., Chem. Fund. 15 (1), 1976, pp 59-64..

Pinyol, N.M., E.E. Alonso and S. Olivella, "Rapid drawdown in slopes and embankments", *Waterresources Research*, 2008.

Pruess, K., C. Oldenburg and G. Moridis, “TOUGH2 User’s Guide, Version 2.0”, Report LBNL-43134, Lawrence Berkeley National Laboratory, Berkeley, Calif., 1999.

Rohmer J. and Bouc O., “A response surface methodology to address uncertainties in cap rock failure assessment for CO_2 geological storage in deep aquifers”, *International Journal of Greenhouse Gas Control* 4, 2010, pp.198-208.

Rutqvist, J. and Tsang, C.F., “TOUGH-FLAC: A NUMERICAL SIMULATOR FOR ANALYSIS OF COUPLED THERMAL-HYDROLOGIC-MECHANICAL PROCESSES IN FRACTURED AND POROUS GEOLOGICAL MEDIA UNDER MULTI-PHASE FLOW CONDITIONS”, PROCEEDINGS, TOUGH Symposium, Lawrence Berkeley National Laboratory, Berkeley, California, 12-14 May, 2003.

Rutqvist, J., Birkholzer, J.T., Cappa, F., Tsang, C.F., “Estimating maximum sustainable injection pressure during geological sequestration of CO_2 using coupled fluid flow and geomechanical fault-slip analysis”, *Energy Conversion and Management*, 48, 2007, pp. 1798-1807.

Rutqvist, J., Birkholzer, J.T., Tsang, C.F., “Coupled reservoir-geomechanical analysis of the potential for tensile and shear failure associated with CO_2 injection in multilayered reservoir-cap rock systems”, *Int. J. Rock Mech. Min. Sci.* 45, 2008, pp. 132-143.

Saaltink, M., Benet, I., Ayora, C., “RETRASO, Fortran Code for Solving 2D Transport of Solutes, User’s guide”, *Barcelona, E.T.S.I. Caminos, Canales y Puertos, Universitat Politecnica de Catalunya and Instituto de Ciencias de la Tierra, CSIC, 1997.*

Saaltink, M.W., Ayora, C., Carrera, J., “A mathematical formulation for reactive transport that eliminates mineral concentration”, *Water Resources Research* 34, 1998, pp. 1649-1656.

Saaltink, M.W., C. Domenech, C. Ayora and J. Carrera, “Modeling the oxidation of sulphides in an unsaturated soil”, *Geological Society, London, Special Publications*, Vol. 198, 2002, pp. 187-204.

Saaltink, M.W., F. Batlle, C. Ayora, J. Carrera and S. Olivella, “Retraso, A code for modeling reactive transport in saturated and unsaturated porous media”, *Geologica acta: an internal earth science journal*, Vol. 2, No. 3, 2004, pp. 235-251.

Saaltink, M.W., C. Ayora and S. Olivella, “User’s guide for RetrasoCodeBright (RCB)”, Department of Geotechnical Engineering and Geo-Sciences, Technical University of Catalonia (UPC), Barcelona, Spain, 2005.

Salvany, J.M., J. Carrera, J. Bolzicco and C. Mediavilla, “Pitfalls in the geological characterization of alluvial deposits: site investigation for reactive barrier installation at Aznalcóllar, Spain”, *Quarterly Journal of Engineering Geology and Hydrogeology*, Vol. 37, 2004, pp. 141-154.

Shipton, Z.K., J.P. Evans, D. Kirschner, P.T. Kolesar, A.P. Williams and J. Heath, “Analysis of CO_2 Leakage through Low-permeability Faults from Natural Reservoirs in the Colorado Plateau, East-central Utah”, *Geological Storage of Carbon Dioxide*, Geological Society, London, Special Publications, 2004, Vol. 233, pp. 43-58.

Soave, G., Chem. Eng. Sci. 27, 1972, pp 1197-1203.

Terzaghi, K., “Erdbaumechanik auf Bodenphysikalische Grundlage”, Franz Deuticke, 1925, Leipzig.

Terzaghi, K. “Theoretical Soil Mechanics”, *John Wiley and Sons*, 1943, New York, USA.

van der Meer, L.G.H., ”CO_2 Storage in the Subsurface”, *Greenhouse Gas Control Technologies*, Vol. I, J. Gale and Y. Kaya (eds.), Elsevier, Amsterdam, 2003, pp. 201-206.

Vidal-Gilbert, S., Nauroy, J.F., Brosse, E., "3D geomechanical modeling for CO_2 geologic storage in the Dogger Carbonates of the Paris Basin", Int. J. of Greenhouse Gas Control 3, 2009, pp. 288-299.

Wigley, T.M.L, Richels, R., and Edmonds, J.A., "Economic and environmental choices in the stabilization of atmospheric CO_2 concentrations", *Nature* 379, 1996, pp. 240-243.

Wiprut, D., Zoback, M.D., "Fault reactivation and fluid flow along a previously dormant normal fault in the northern North Sea", *Geology* 28, 2000, pp. 595-598.

Zheng, D. Q., Guo, T. M., Knapp, H., "Experimental and modeling studies on the solubility of CO_2, CHClF2, CHF3, C2H2F4 and C2H4F2 in water and aqueous NaCl solutions under low pressures", *Fluid phase equilibra*, vol 129, 1997, pp. 197–209.

Zoback, M.D., Ross, H. and Lucier, A., "Geomechanics and CO_2 Sequestration", *GCEP Technical Report*, Stanford Univ., Global Climate and Energy Project, 2006.